

**Fu Foundation School of
Engineering and Applied Science
Presents the Sixth Annual**

SENIOR DESIGN '19
EXP



**Thursday, May 9th | 12pm-3pm
Roone Arledge Auditorium
Columbia University**



To view projects from previous years, visit:

<https://studentresearch.engineering.columbia.edu/content/senior-design-expo>

Welcome to Columbia University's 6th annual Senior Design Expo organized by the Fu Foundation School of Engineering and Applied Science.

As a culmination of their education at Columbia Engineering, students undertake projects in their senior year to test their engineering mettle. Students form groups, identify a real-world problem and, over the course of the academic year, develop working prototypes or detailed design studies to solve those problems. Groups also receive dedicated mentorship from faculty along their arduous journey that has brought them to this Expo today. The spirit of Engineering for Humanity is exemplified in their efforts to make the world a better place.

This year we have almost 60 groups representing the breadth and depth of Columbia Engineering who are excited to share their solutions with you. Groups have developed new methods of characterizing materials and even engineered greener materials for consumer products and more environmentally friendly cements. An engineering and economic analysis for producing methanol from syngas as a byproduct of electricity generation demonstrates its economic feasibility. Selection of hybrid crops for demanding environmental conditions has traditionally been a slow process, but with modern modeling techniques, crop-yield can be increased more rapidly to meet population demands. Improving the built environment can significantly reduce the carbon footprint of our urban environment; and multiple groups have proposed modern designs for NYC buildings, including those on the Columbia University campus, for lower environmental impact and greater comfort. Several groups have undertaken the challenge to provide novel solutions to improve health, including a device that uses acoustic vibrations to clear lungs of obstructions. Others have been rehabilitating historic musical instruments as well as exploring music composition with modern electronics, while others are thinking creatively about next-generation transportation including robust designs for exploring alien worlds.

I encourage you to explore the Senior Design Expo and speak to the students to learn more about their exciting solutions to real-world problems – our students are doing amazing things!

Barclay Morrison
Vice Dean of Undergraduate Programs
Professor of Biomedical Engineering

APPLIED PHYSICS AND APPLIED MATH

Towards Automated Materials Characterization: Non-negative Matrix Factorization and Data Clustering

Sasaank Bandi
Pages 9-10 | Table 1

Grain Size and Grain Boundary Character Distributions of Al-Mn Films

Mehrzad Farnoosh, Benjamin McCaffrey
Page 11 | Table 2

Combatting Tradeshow Pollution with Bacterial Cellulose and Native American Textile Treatment Processes

Christian Joseph
Page 12 | Table 3

Effect of Microstructure on the Resistivity of Thin Film Tantalum

Abraham Oh
Page 13 | Table 4

Copper Pigment Degradation in Early European Printed Books

Aren Small
Page 14 | Table 5

Identifying Diels-Alder Reactions for High-Heat-Capacity Organic Thermal Fluids Using Density Functional Theory

Evan Spotte-Smith
Page 15 | Table 11

Creating Carbon Free Cement: Using Rheology to Find Role of Calcium in Fly Ash and Slag Systems

Donald Swen
Page 16 | Table 12

BIOMEDICAL ENGINEERING

Homer101

Samuel Castro, Mary Grace Gana, Shirley
Xian, Miriam Saffern, Amy Wu
Page 18 | Table 6

Vicious Cycle

Changhee Lee, Katherine Strong, Sarah
Nick, Srinidhi Bharadwaj, Yuge Xiao
Page 18 | Table 7

PneumoTech

Janice Chung, Yihuai Qu, Joanna Zhang,
Joyce Zhou, Tiffany Li
Page 19 | Table 8

BUDI

Blynn Shideler, Elizabeth Shrout, Rachel
Alexander, Katherine Cavanaugh
Page 19 | Table 9

Hera

Kelly Ryu, Mia Saade, Rachel Mintz,
Stephanie Rager
Page 20 | Table 10

DiaCam

Temitope Akinade, Perla Canales, Daniel
Solis, Chisomam Osuji, Walker Magrath
Page 20 | Table 14

XZAMN

Nicole Boyd, Michelle Feely, Aaron
Maccabee, Xin Xiong, Zhener Zhang
Page 21 | Table 15

VisaVein

Saiti Halder, Luke Thorsell, Zarmeen
Mussa, Aubrianna Queen
Page 22 | Table 17

Stroke Alert

James Gornet, Robin Guo, Minyong Jung,
Destiny Machin, Lindsay Testa
Page 21 | Table 16

CEA Solution

Diana Lu, Emily Chen, Leah Zeng, Lorenzo
Talbot-Foote, Maveric Abella
Page 22 | Table 18

CHEMICAL ENGINEERING**Natural Gas to Methanol Production Plant**

Daniela Marin, Shirley Xu
Page 24 | Table 13

CIVIL ENGINEERING**Fueled by the Elements: A Solar-Powered
Resort**

Bailey Alexander, Samantha Grech, Tracy
Paltoo, Carly Press, Abigail Thomas
Page 26 | Table 21

New Cape Cod Bridge

Christopher Defalco, Bryan Lei, Geyang
Zhou, Jessie Yan
Page 28 | Table 23

The Prism

Lorenzo Ferrari, Salomon Dayan, Marco
Della Genco, William Masters
Page 27 | Table 22

Amazon HQ2

Isabel Neiva, Katherine Burt, Lin Ge, Min
Young Hwang, Eleanor Rassbach
Page 29 | Table 24

San Francisco World Cup Stadium

Carolina Garcia, Andrew Hathaway,
DeWein Pelle, Yue Yu, Yifan Zhou
Page 30 | Table 25

EARTH AND ENVIRONMENTAL ENGINEERING

**The Impact of Climate Change on Cities:
Investigating the Urban Heat Island
Effect in Chicago, New York, and Durban**

Priscilla Bell, Amit Krishnan, Eleni
Reynolds, Nicole Romola

Pages 32-33 / Table 27

**Retrofitting Heating and Cooling Systems
with Variable Refrigerant Flow System
on Columbia University's Morningside
Campus**

Iris Lin, Andrew Jeon, Yueli Liang, Yukun
Yang

Page 34 / Table 28

**Water Reclamation and Salinity
Abatement: A feasibility survey to
implement potable reuse in Manalapan,
NJ**

Ansley Carlisle, Zoe Berry, Rachel Lujan

Page 35 / Table 29

**Save the Trout! Framework for the Cold
Water Releases in the Delaware River
Watershed**

Rachel Barkowitz, Daniel Dray, Lillianne
Farih, Heather Morriss

Page 36 / Table 30

ELECTRICAL ENGINEERING

**A Baseball Strike Zone Delineator
Implemented Using Digital Image
Processing Techniques**

Joon Mo Park

Pages 38-39 / Table 31

Dual-Axis Interactive Base
Matthew Barlow, Christopher Bhim,
Marielle Jones, Luis Perez, Neel Singal

Page 40 / Table 32

**Frequency Stabilization and External
Control Module for the Buchla 100
Analog Music Synthesizer**

William Mauro

Page 41 / Table 26

Chaotic DJ

Ryan Arteaga, Jinglei Guo, Ishraq
Khandaker, Hongyi Li

Pages 42-43 / Table 33

**Homemade Single-Supply Class D
Amplifier w/ Bluetooth**

Jay Mok, Chase Stine

Page 44 / Table 49

**Semi-Parametric Equalizer using 20
Bands for Creating Arbitrary Frequency
Responses**

Jose Rubianes

Page 45 / Table 50

Logic Board

Leah Feuerman, Jacqueline Napolitano,
 Sayaan Nawaz, Jackson Welles

Page 46 / Table 51

**Modular Micropower Electronics for
 Fully Inte-grated Energy Storage
 Compatible with a Vari-ety of Storage
 Media**

Peter Frey, Michael Harriss, Johnny Li, Max
 Moeller

Page 47 / Table 52

Pet Minder

Benjamin Brigman, Asher Goldfinger,
 Anthony Gutierrez, Moises Pena Jr., Ryan

Davies

Page 48 / Table 53

Smart Walker and Boot

Shamirah Tillman, Mohammad Khojah

Page 49 / Table 48

**The AWG short-reach (1<km) optical
 link**

Runjia (Luna) Zhang

Pages 50-51 / Table 54

Junior Class Project

Table 55

INDUSTRIAL ENGINEERING & OPERATIONS RESEARCH/COMPUTER SCIENCE

Football Simulator 2019

Thomas Mecattaf, Mohnish Chakravarti,
 Cameron Terry

Page 53 / Table 19

**Predicting Crop Yield in North America:
 Modeling Corn Hybrid Performance and
 Farmer Centered Pipelines**

Alysha Hudson

Page 54 / Table 20

MECHANICAL ENGINEERING

PreSpice Automated Spice Cabinet

Sara Cummings, Connor Johnston, Joshua
 Katz, Brandon Kubick, David Reyes

Page 56 / Table 35

STASIS x citibike

Nathaniel Fisher, Peter Hidley II, Chase
 Pipkin, Travis Pulliam

Pages 58-59 / Table 47

InstaSorg

Quincy Delp, Chengke Fan, Jason Fan, Yifei
 Tian, Victoria Wang

Page 57 / Table 36

IoT Tensegrity Tumbleweed

Leonardo Aquino Alves Belmar da Co,
 Luke Gile, Steven Hyland, Breanna Johnson

Page 60 / Table 37

Shred-It

Racquel Glickman, Riley Greene, Molly Hazlehurst

Page 61 / Table 38

iPothecary

Yeil Choi, Christian Puerta, Elijah Schultz, Cory Ye

Page 62 / Table 39

The Ark

Liam Dwyer, Mark Hellinger, Kirsten McNeill, Andrew Moshova, Patrick Naughton

Page 63 / Table 41

A Non-slip Continuously Variable Transmission for a Bicycle

Max Holschuh, Nikolay Ionkin, Mingxin Jia, Graham Maxwell, William Zhang

Page 64 / Table 40

FSAE EV Systems Integration

Katherine Guan, Austen Paris, Fernando Pascual-Marquez, Henry Tucher

Pages 65-66 / Table 42

Shoe Tying Robot

Rafael Corrales-Fatou, Eric Li, Arturo Mori Beltran, Cesar Trujillo

Page 67 / Table 43

PLASTICS

Erik Boyle, Thomas Orr, Jose Pablo Rueda Molina, Aaron Thompson

Page 68 / Table 46

CulpeoWASH

Adeel Ahmad, Onur Calikusu, Christopher Fryer, Charles Johnson

Page 69 / Table 44

Card Dealer 3000

Andrew DePerro, Connor Finn, John Michael Long, Brian Nicholas

Page 70 / Table 45

VTOAL Aircraft

Simon Anuszczyk, Rebecca Brunsberg, Haeyeon Jang, John Pederson Jr., Lily Zhao

Page 71 / Table 34

APPLIED PHYSICS & APPLIED MATH

Towards Automated Materials Characterization: Non-negative Matrix Factorization and Data Clustering

Sasaank Bandi, Simon J. L. Billinge

Solutions to many of the challenges society faces will require new materials. These materials will have to exhibit properties that make them suited to function in conditions that previously were unimaginable. Technological developments have led to experimental tools that can measure these properties in a fraction of a second, inevitably leading to the production of large volumes of data [1, 2]. Since a material's properties are determined by its structure, x-ray diffraction is one of these powerful tools in screening materials for extraordinary properties. To speed up this screening process, it is imperative to develop techniques to analyze diffraction data quickly and autonomously.

Two such techniques have been studied during the course of this project to facilitate the rapid characterization of diffraction data: Agglomerative Hierarchical Clustering [3] (AHC) and Non-negative Matrix Factorization [4] (NMF). Both have been shown to have utility in various circumstances. In the case of AHC, large volumes of data are grouped into k clusters depending on their similarity to each other. A researcher may then analyze a few data points from each cluster, greatly saving time over analyzing the entire set, whilst gaining an good understanding of the dataset as a whole. An example of the results of a clustering experiment is illustrated in Fig. 1

On the other hand, NMF breaks down the dataset into representative elements and determines how to linearly combine these elements to recreate every data point in the dataset. This proves to be useful when analyzing a dataset in which one structure is changing into another (due to heat, pressure, etc.). In this case, NMF would output a representation of both structures, and provide information about when the transformation occurred.

Both methods were tested on simulated datasets of 1000 randomly generated PDFs from three distinct crystal structures as well as experiments capturing the growth of Silver Nanoparticles and the temperature driven structural changes in methylammonium lead bromide (MAPbBr₃). Both performed well on the simulated dataset, being able to sort the data into three structural categories with less than 5% error in a matter of minutes. In the experimental dataset, the clustering method was not able to sort the data into stable clusters. However, NMF was able to identify the structures that were present and how they evolved as a function of the independent variable, allowing the experimenter, in principle, to follow the experiment without any prior data analysis.

- [1] P. J. Chupas, K. W. Chapman, and P. L. Lee, Applications of an amorphous silicon-based area detector for high-resolution, high-sensitivity and fast time-resolved pair distribution function measurements, *J. of Appl. Crystallogr.* 40, 463 (2007).
- [2] P. J. Chupas, M. F. Ciruolo, J. C. Hanson, and C. P. Grey, In situ x-ray diffraction and solid-state NMR study of the fluorination of Al₂O₃ with HCF₂Cl, *J. Am. Chem. Soc.* 123, 1694 (2001).
- [3] G. J. Szekely and M. L. Rizzo, Hierarchical clustering via joint between-within distances: Extending ward's minimum variance method, *J. Classification* 22, 151 (2005).
- [4] D. D. Lee and H. S. Seung, Learning the parts of objects by non-negative matrix factorization, *Nature* 401, 788 (1999).

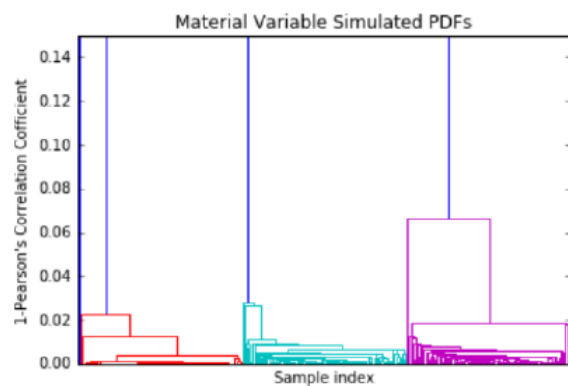


FIG. 1: Results of hierarchical clustering on randomly simulated data from three crystal systems. 1000 samples are automatically grouped (by colored linkages) into three categories.

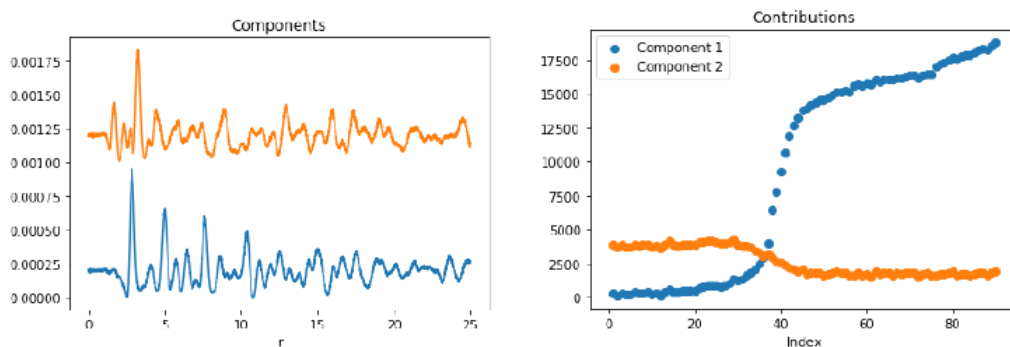


FIG. 2: Results of NMF on Ag nanoparticle growth in zeolite support. (Left) The two components found by NMF which resemble PDFs of real phases. (Right) The evolution of the amounts of the two contributions as the experiment progressed.

Grain Size and Grain Boundary Character Distributions of Al-Mn Films

Benjamin McCaffrey, Mehrzad Farnoosh

Advisor: Prof. Katayun Barmak

Materials Science and Engineering Program

Precession electron diffraction-based crystal orientation mapping data of an Al film were re-processed and re-analyzed to re-establish the procedure for reliable processing of new mapping data. The new mapping data of an annealed Al-Mn film are used to obtain the grain size and grain boundary character distributions, with the aim of gaining insight into the structure-superconducting transition edge behavior of Al-Mn alloys.

Background

Doping Al films with small amounts ($<0.5\text{at}\%$) of Mn has proven very successful in reducing noise in superconducting transition edge sensors for sensitive photon detection in the submillimeter, optical and x-ray regimes [1]. In preparation for the analysis of the Al-Mn samples sent from the National Institute of Standards and Technology, Boulder, CO, results from previous work by Barmak and Rohrer were re-processed and re-analyzed to re-establish a reliable procedure necessary for the current study [2, 3]. Example precession electron diffraction patterns of an Al film obtained in the transmission electron microscope (TEM) are shown, in Fig. 1 [3].

These diffraction patterns were then indexed by matching them with precalculated patterns [2, 3]. These indexed files could then be viewed as inverse pole figure (IPF) maps, as shown in Fig 1. These IPFs provide information on orientation of each crystallite, or grain, in the sample [4].

These IPFs could then be cleaned and used to obtain grain size distribution, and grain boundary character distribution (GBCD) [4]. GBCD is important, because it provides a complete description of the distribution of crystallite orientations, grain boundary misorientation, and orientations of grain boundary planes [4, 5].

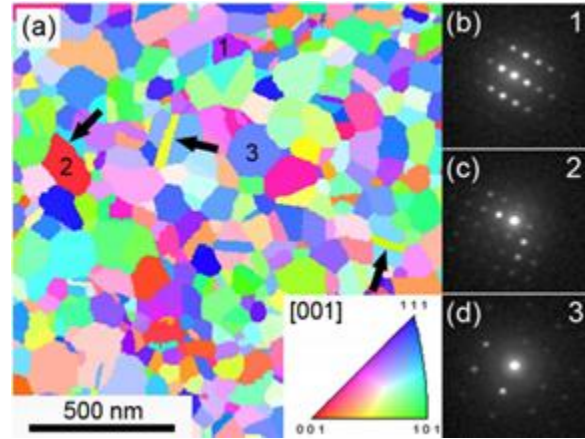


Figure 1. Inverse pole figure map, and related spot diffraction patterns of thin aluminum film (from previous work done in [3]).

Acknowledgements

The students would like to thank NIST, Profs. Barmak, Billinge and Rohrer, and Drs. Liu, Zangiabadi and Kelly for guiding this study.

References

1. Deiker SW, Doriese W, Hilton GC, Irwin KD, Rippard, WH, Ruggiero ST, Williams A, Young BA, (2004) Superconducting transition edge sensor using dilute AlMn alloys, *Appl. Phys. Lett.*, 85:2137-2139.
2. Barmak K, Eggeling E, Kinderlehrer D, Sharp DR, Ta'asan S, Rollett, AD, Coffey KR, (2013) Grain growth and the puzzle of its stagnation in thin films: The curious tale of a tail and an ear, *Prog. Mater. Sci.* 58:987–1055.
3. Rohrer GS, Liu X, Liu J, Darbal A, Kelly MN, Chen X, Berkson MA, Nuhfer NT, Coffey KR, Barmak K (2017) The grain boundary character distribution of highly twinned nanocrystalline thin film aluminum compared to bulk microcrystalline aluminum. *J. Mater. Sci.* 52:9819–9833.
4. Barmak K, Coffey K (2016) *Metallic films for electronic, optical and magnetic applications: structure, processing and properties.* Woodhead Publishing
5. Saylor DM, Morawiec A, Rohrer GS (2003) Distribution of grain boundaries in magnesia as a function of five macroscopic parameters. *Acta Mater.* 51:3663–3674.

Combatting Tradeshow Pollution with Bacterial Cellulose and Native American Textile Treatment Processes

Christian Joseph

Advisors: Professor Theanne Schiros & Professor

Simon J. L. Billinge

Materials Science and Engineering Program

Tradeshows in the U.S. generate over 600,000 tons of landfill waste each year [1] , where the materials release greenhouse gases as well as harmful chemicals used in their manufacture. For tradeshows, these chemicals include flame retardants required for large events, which are related to a myriad of health issues. In 95% of U.S. families, the EPA detected flame retardants linked to thyroid disorders, learning disabilities, hyperactivity, hearing and memory problems, reproductive problems, birth defects, and possibly cancer [2] .

Bacterial cellulose (BC) is a promising biodegradable material that can be grown to shape from sugar waste streams. Using Native American tanning techniques, we have created water resistant, flame retardant, strong and flexible BC with promise for a range of applications, including non-toxic, compostable, materials for trade show displays with a closed-loop life cycle. Electronic capability, such as sensing and lighting, is introduced with circuits created from conductive screen printing ink, with electronic components that can be easily removed and interchanged.

Background

Biocouture led by Suzanne Lee first explored the use of BC as a textile. However, inherent materials challenges, including lack of water resistance and brittleness after drying have limited direct translation of BC to fabric and textiles [3] . The Schiros group has found that treating dried BC with indigenous tanning and smoking techniques result in water resistance and extreme flame retardance. This makes dried BC an excellent candidate for a sustainable, flame resistant trade show display material.

G. xylinus bacteria strains can synthesize cellulose through the metabolism of sugars and alcohols [4].

We cultured a symbiotic colony of bacteria and yeast (SCOBY) , allowing it to ferment sugars and alcohols to spin nano-cellulose fibres, which grew layer by layer to produce a thick mat of cellulose taking the shape of the container's cross-section [5] . BC readily absorbs natural color from plants. This allows for non-toxic customization of visually appealing display design. The cellulose can be dried and treated with indigenous in order to obtain desired mechanical properties and requisite flame retardance. Finally, we printed circuits the conductive ink demonstrating the feasibility of implementing electronic components in this bio textile. The final product is a flexible, strong, non-toxic tradeshow display with a closed loop life cycle that addresses the problems of environmental destruction and public health while incorporating electronic components via conductive screenprinting.

Acknowledgements

I would like to thank Professors Schiros, Billinge, and Goetz. I would also like to thank Shanece Esdaille, Romare Antrobus, Adrian Chitu, Amirali Zangiabadi, and Karen Sanchirico

References

[1] "Exploring Environmentally Friendly Trade Show Options." *Derse*. September 08, 2016. Accessed October 15, 2018. <https://derse.com/exploring-environmentally-friendly-trade-show-options/>.

[2] Mireia Gascon, Martine Vrijheid, David Martínez, Joan Fornas, Joan O. Grimalt, Maties Torrent, Jordi Sunyer, Effects of pre and postnatal exposure to low levels of polybromodiphenyl ethers on neurodevelopment and thyroid hormone levels at 4 years of age, *Environment International*, Volume 37, Issue 3, 2011, Pages 605-611, ISSN 0160-4120, [3] Ehrhardt, Anelise & Groner, Sibylle & Bechtold, Thomas. (2007) . Swelling Behaviour of Cellulosic Fibres – Part I: Changes in Physical Properties. *Fibres and Textiles in Eastern Europe*. 15. 64-65.

Effect of Microstructure on the Resistivity of Thin Film Tantalum

Abraham Oh

Kwang Taeg Rim, James Im

This paper investigates the effects of grain microstructure and orientation on the conductivity and resistivity of thin film Tantalum. Tantalum forms a thin protective oxidized layer that protects it from further oxidation. This thin oxidized layer is also very stable over a wide range of temperatures. This means that Tantalum is very resilient and does not degrade easily over time. Combined with the high dielectric constant of its thin oxide layer, it is suitable for use in a variety of electrical devices such as phones.

A continuous wave (CW) laser ($\lambda=532\text{nm}$), with a spot size of 200 to 400 μm at 5W, is used to crystallize the thin film Tantalum. The laser is used to locally melt the Tantalum throughout its thickness so that the Tantalum can recrystallize into larger grains with a more uniform orientation texture. The laser is operated at 5W with 1 scan per line to melt and recrystallize the Tantalum. After each scan, Electron Back Scattered Diffraction (EBSD) and Scanning Tunneling Microscopy (STM) were utilized to analyze the microstructure of the grain (size, orientation) and grain boundaries. This allows us to observe the microstructure evolution of the Tantalum over each scan. The results were analyzed using the Johnson-Mehl-Avrami-Kolmogorov equation as a potential tool to enable us to predict the further evolution of the microstructure.

We observe, that over time, the grains start to orient in the $\langle 001 \rangle$ direction and the grains in the $\langle 001 \rangle$ direction grow larger after each scan. After several scans, a 4-point probe was employed to measure the resistivity of the particular texture.

Preliminary results indicate that grain orientation and microstructure greatly affect conductivity/resistivity.

References

- [1] A.S.H. Van der Heide; J.H Bultman; M.J.A.A. Goris; J. Hoornstra, Influence of grain orientation on contact resistance at higher emitter resistances, investigated on alkaline and acid saw damage removal, 3rd World Conference on Photovoltaic Energy Conversion, May 11-18, 2003.
- [2] W, Ying, Investigation of Melting and Solidification of Thin Polycrystalline Silicon Films via Mixed-Phase Solidification, Doctoral thesis, Columbia University, 2016.

Copper Pigment Degradation in Early European Printed Books

Aren Small

Advisor: Professor Katayun Barmak
Alexis Hagadorn and Emily Lynch
Columbia University Libraries, Columbia University

Abstract

In this project the aging of copper carbonate based pigments on paper was simulated and the aging products were characterized. The aim of these studies to develop improved methods for conservation of European early books.

Incunabula, or European books printed before 1500 often had hand painted illustrations and lettering which were painted with copper carbonate based green and blue pigments. Over time, these pigments and the underlying paper have degraded and this is believed to be caused by factors such as pH, temperature and relative humidity.

In this project, the aging process of incunabula was simulated using samples of Azurite (blue) and Malachite (green) pigment, mixed with two types of binders, on paper and by subsequently aging the samples at either high or low temperature. The pH of the pigment-binder solutions was also varied. The products of the artificial aging process were then characterized using Raman spectroscopy by measuring spectra and comparing the measured spectra to references to identify what was present. Samples were also imaged using optical microscopy.



Figure 1. The reverse side (verso) of an incunabula, showing the degradation of the pigment. It was originally blue. (Figure reproduced from Hagadorn, 2004)

Acknowledgements

AS would like to thank Professor Billinge and Michael Berkson.

References

- Hagadorn, Alexis. "An Investigation into the Use of Blue Copper Pigments in European Early Printed Books". *Book and Paper Group Annual* 23:41-55. (2004)
- Gutzcher, Daniel et al. "Conversion of Azurite into Tenorite". *Studies in Conservation* 34.3:117-122. (1989)

Identifying Diels-Alder Reactions for High-Heat-Capacity Organic Thermal Fluids Using Density Functional Theory

Evan Walter Clark Spotte-Smith^{1,2}, Peiyuan Yu²,
Anubhav Jain², Ravi S. Prasher^{2,3}

¹Department of Applied Physics and Applied
Mathematics, Columbia University

²Energy Technologies Area, Lawrence Berkeley
National Laboratory

³Department of Mechanical Engineering, University
of California, Berkeley

Heat is a dominant component of energy consumption in industrial and household settings, with over 90% of total global primary energy being used or wasted on heating.[1] The significance of heat in the energy economy motivates study in methods to capture, transfer, and release thermal energy, allowing not only for effective temperature regulation but also for the recycling of waste heat from thermal processes. Existing thermal storage and transfer technologies that store heat via non-covalent interactions are generally limited in terms of heat capacity and energy storage density.[2] Liquid-phase thermochemical systems, which release and store energy through the formation and breaking of covalent bonds, are promising both because they typically possess high energy densities [3] and because they can be conveniently integrated into many typical thermal transport designs.

Here, we use computational techniques to identify and analyze organic thermal fluids with thermal properties enhanced by the dissolution of Diels-Alder [4 + 2] cycloaddition reactions. The Diels-Alder reaction family had previously been suggested as a class of thermal energy storage materials by Lenz [4] and Poling.[5] These reactions possess high reaction enthalpy and entropy, resulting in considerable heat capacity enhancement at moderate temperatures.

Diels-Alder reactions from the Reaxys database [6] were pre-screened and ranked based on the boiling points, melting points, vapor pressures, aqueous solubilities, and octanol-water partition coefficients of the reactant molecules, as predicted by EPI Suite.[7] Based on this ranking, a set of 16 reactions was selected for analysis. Reaction thermodynamics (ΔH , ΔS , $T^* = \Delta H/\Delta S$), solubility (S) and thermal properties (C_p , ES) were predicted using density functional theory (DFT) at ω B97X-D/6-311++G(d,p)// ω B97X-D/6-31G(d) level of theory. The SMD model [8] was used to model the solvation of the reactant molecules in Dowtherm A, a common organic thermal fluid.[9]

Of the reactions screened by DFT, four are predicted to have a turning temperature T^* in the

working range of Dowtherm A (12 – 257 °C). Two are predicted to be soluble in Dowtherm A, and one is predicted to have a maximum specific heat capacity of 7.89 J/cm³-K and a volumetric energy density of 0.944 MJ/L, a gain of 103.3% over the base solvent. To our knowledge, this reaction has one of the highest heat capacities of any organic thermal fluid.

Acknowledgments

This research used resources of the National Energy Research Scientific Computing Center, a DOE Office of Science User Facility supported by the Office of Science of the U.S. Department of Energy under Contract No. DE-AC02-05CH11231. It was supported by the Laboratory Directed Research and Development Program (LDRD) at Lawrence Berkeley National Laboratory under contract No. DE-AC02-05CH11231. Samuel Blau was greatly helpful in designing and troubleshooting computational workflows in Q-Chem. Simon Billinge provided useful feedback throughout this project.

References

- [1] I. Gur, K. Sawyer, R. Prasher, *Science*. **2012**, 335, 1454- 1455.
- [2] A. H. Abedin, M. A. Rosen, *The open renewable energy journal*. **2011**, 4, 591-610.
- [3] P. Pardo, A. Deydler, Z. Anxionnaz-Minvielle, S. Rougé, M. Cabussud, P. Cognet, *Renewable and Sustainable Energy Reviews*. **2014**, 32, 591-610.
- [4] T. G. Lenz, L. S. Hegedus, J. D. Vaughan, *International Journal of Energy Research*. **1982**, 6, 357-365.
- [5] B. E. Poling, *DOE Solar Storage Workshop*. **1979**.
- [6] B. Sjoeborg, *Database Reaxys*.
- [7] U.S. E.P.A. *Estimation Programs Interface Suite for Microsoft Windows*, v 4.11. **2012**.
- [8] A. V. Marenich, C. J. Cramer, D. G. Truhlar, *The Journal of Physical Chemistry B*. **2009**, 113, 6378-6396.
- [9] Dowtherm a heat transfer fluid. *Product technical data*, 1997.

Creating Carbon Free Cement: Using Rheology to Find Role of Calcium in Fly Ash and Slag Systems

Donald Swen

Advisors: Dr. Shiho Kawashima, Dr. Arnaud Castel (UNSW), Dr. Simon Billinge

Cement production currently accounts for 7% of global CO₂ emissions.¹ To produce cement, calcium carbonate (limestone) must be heated at high temperatures of 1500 C to turn into calcium oxide, releasing CO₂ in the process. With demand for ordinary Portland cement (OPC) in developing countries projected to double by 2050, a search for alternative, eco-friendly cement binders is being carried out.^{2 3}

Geopolymeric cement is one such area of increasing interest due to its potential in reducing CO₂ emissions by 44-64%⁴ compared with OPC and reutilizing power plant waste such as fly ash and bottom ash waste. The process involves the alkaline activation of aluminosilicates (such as kaolin, metakaolin, and coal ash), releasing aluminate and silicate species that polymerize and form gel networks that harden⁵. The result is a superior cement binder⁶.

In collaboration with Dr. Arnaud Castel from UNSW, we studied the role of calcium in forming calcium silicate hydrate gel networks and how that formation affects aluminosilicate gel formation in the same system through probing the early age properties of cement through shear rheology to give yield stress, viscosity, and modulus evolution. Similar studies have been carried out for metakaolin systems⁷ and potassium hydroxide system⁸. Here, we investigated (50% fly ash /50% slag) and (25% fly ash /75% slag) systems with three different alkaline concentrations (Na₂O%) each. To supplement our research, we observed the crystalline degrees in each system using synchrotron x-ray diffraction for the same early age time scale. X-ray fluorescence was used to determine the chemical composition of fly ash and slag.

Conducting a thorough rheological study helps to understand the mechanisms of how different compositions of slag and fly ash with different levels of alkaline activation effect gel formation, microstructure (porosity), and strength. Further, it helps fill a current knowledge gap, where the rheological behavior of geopolymers, although distinctly different from that of conventional Portland cement systems, is not well understood. Better

understanding and control of rheology and workability (general term describing the ease with which fresh concrete mixes can be cast during construction while maintaining suspension stability) can contribute to its possible future adoption as a material to decrease global carbon emissions.

References

- 1 Meyer, C. (2009). The greening of the concrete industry. *Cement and concrete composites*, 31(8), 601-605.
- 2 Pacheco-Torgal, F., Moura, D., Ding, Y., & Jalali, S. (2011). Composition, strength and workability of alkali-activated metakaolin based mortars. *Construction and Building Materials*, 25(9), 3732-3745.
- 3 US Geological Survey. (n.d.). Major countries in worldwide cement production from 2012 to 2017 (in million metric tons). In *Statista - The Statistics Portal*.
- 4 McLellan, B. C., Williams, R. P., Lay, J., Van Riessen, A., & Corder, G. D. (2011). Costs and carbon emissions for geopolymer pastes in comparison to ordinary portland cement. *Journal of cleaner production*, 19(9-10), 1080- 1090.
- 5 Liew, Y. M., Heah, C. Y., & Kamarudin, H. (2016). Structure and properties of clay-based geopolymer cements: A review. *Progress in Materials Science*, 83, 595- 629.
- 6 Duxson, P., Provis, J. L., Lukey, G. C., Mallicoat, S. W., Kriven, W. M., & Van Deventer, J. S. (2005). Understanding the relationship between geopolymer composition, microstructure and mechanical properties. *Colloids and Surfaces A: Physicochemical and Engineering Aspects*, 269(1-3), 47-58.
- 7 Steins, P., Poulesquen, A., Diat, O., & Frizon, F. (2012). Structural evolution during geopolymerization from an early age to consolidated material. *Langmuir*, 28(22), 8502- 8510.
- 8 Puligilla, S., & Mondal, P. (2013). Role of slag in microstructural development and hardening of fly ash-slag geopolymer. *Cement and Concrete Research*, 43, 70-80.

BIOMEDICAL ENGINEERING

Homer101

*Samuel Castro, Mary Grace Gana, Miriam Saffern, Amy Wu, Shirley Xian
Advisors: Dr. Peter Yim, Prof. Clark Hung*

Out-of-theater intubations by non-expert intubists are associated with failure rates as high as 49%. Failure to intubate may result in hypoxia, hypotension, and even death. Vocal cord visualization is essential for tube placement and breathing restoration. This is facilitated by correct placement of a laryngoscope blade in the vallecula to lift up the epiglottis and visualize the vocal cords inside the trachea. Therefore, there is a need for a way to quickly and accurately guide the laryngoscope blade correctly into the vallecula in out-of-theatre settings. Homer101 aims to create a “smart” laryngoscope blade that guides the less-experienced intubist through tactile sensing mechanisms. By attaching force sensors to the blade and processing resulting data, the intubist receives real-time feedback on blade placement. Initial testing in training sessions with attending anesthesiologists shows that 89% of incorrect intubations can be detected, thus improving the sensitivity of the procedure.

Vicious Cycle

*Srinidhi Bharadwaj, Changhee (Stephen) Lee, Sarah Nick,
Katherine Strong, Yuge Xiao
Advisor: Prof. Christoph Juchem*

Bronchiectasis is an irreversible lung deterioration that leads to mucus buildup in the airways. Bronchiectasis is a chronic condition, trapping patients in a vicious cycle of inflammation and infection. Bronchiectasis care primarily focuses on mucus clearance through manual chest physiotherapy and assistive clearance devices. However, treatments frequently fail due to poor patient compliance stemming from time limitations and a lack of device adaptability. Patients need a treatment option that provides greater portability, adaptability, and comfort. The VC Woofer is a hands-free device that facilitates airway clearance through acoustic vibrations to the chest. The VC Woofer is fitted with an adjustable harness, a padded coupler, and a rechargeable battery for comfortable and portable use. Initial prototype testing demonstrated significantly greater mucus clearance with the VC Woofer than with three existing mucus clearance devices. Thus, the VC Woofer provides an alternative airway clearance method for patients who struggle to comply with their current treatment.

PneumoTech

*Janice Chung, Tiffany Li, Jess Qu, Joanna Zhang, Joyce Zhou
Advisors: Prof. Samuel Sia, Prof. Gordana Vunjak-Novakovic*

Ventilator-associated pneumonia (VAP) is one of the most common and deadly infections, accounting for 60% of all deaths due to hospital-related infections. Endotracheal tube (ETT) intubation allows for bacterial entry into the lungs, which can result from bacterial biofilm formation inside the ETT or leakage of bacteria-containing subglottic secretions past the ETT cuff. Existing methods of VAP prevention are not standardized, prone to healthcare provider noncompliance, and do not directly address the causes of VAP. PneumoTech addresses the problem of ETT-based infections through a multimodal solution: a UVC fiber bundle for prevention of biofilm formation, a suction system for continuous removal of subglottic secretions, and an automated pressure-regulating cuff for preventing leakage of subglottic secretions. Together, our system effectively targets both causes of VAP, providing a comprehensive and intuitive solution to combat this hospital-based infection.

BUDI

*Katherine Cavanaugh, Rachel Alexander, Elizabeth Shrouf, Blynn L Shideler III
Advisor: Prof. Katie Reuther*

Cerebral palsy (CP) is the most common childhood motor disability. Of the various types of CP, most cases present as spastic hemiplegia--high muscle contracture that affects one side of the body. Those with hemiplegic CP experience great difficulty performing tasks requiring bilateral manipulation and tend not to use their impaired limbs. Upper limb neglect yields clinical consequences including muscular atrophy, limited range of motion, and decreased self-confidence. While leading occupational therapies improve upper limb functionality, hemiplegic patients tend to regress to using the unimpaired arm in the absence of clinicians, and improvements made during therapy are lost. Our BUDI system solves this problem by tracking the movements of the impaired arm. BUDI alerts the user during periods of inactivity through a biofeedback mechanism and displays movement data and progress on an easily-understood platform, ultimately encouraging wearers to use their impaired arm more in daily life.

Hera

Rachel Mintz, Stephanie Rager, Kelly Ryu, and Mia Saade

Advisor: Prof. Kristin Myers

Mastitis is inflammation of breast tissue in breastfeeding mothers due to milk stasis and resultant bacterial infection. The first signs of mastitis are temperature elevation and erythema in the breast(s). These symptoms can quickly progress to intense pain, fever, and chills, followed by possible abscess formation. Mastitis is reported in up to 33% of lactating mothers, yet it often goes undiagnosed until symptoms become severe. Therefore, we developed a device for early detection of mastitis to minimize pain and prevent unwanted cessation of breastfeeding. Our two-part system consists of the Hera Smart Bra and Hera Mobile Application. The bra can accurately measure breast temperature at multiple locations and wirelessly transmit this data to our mobile application. The application displays temperature data in real time and alerts mothers to trends that may be indicative of preclinical mastitis. Mothers can then work to relieve inflammation at home or seek medical treatment before symptoms progress.

DiaCam

Tope Akinade, Perla Canales, Walker Magrath, Chiso Osuji, Daniel Solis

Advisor: Prof. Kristen Myers

Hospital admission during early labor is associated with an increased risk of dystocia, a difficult birth caused by several factors such as the failure of the cervix to contract and expand normally. This leads to an increased risk of medical interventions and adverse outcomes in deliveries. The most critical aspect of labor is diagnosing when the active phase of labor, which occurs at dilation levels between 4 cm and 6 cm. At this point, a delivering mother should be admitted into a labor unit. 60% of laboring low-risk women are sent home for not having started active labor and many express uncertainty about when to return. What is needed is an at-home solution that assists expectant mothers and their care-providers in determining when active labor has begun. DiaCam is a diaphragm-mounted insert containing a mini-camera that monitors cervical dilation during early labor. The images captured by the camera are wirelessly transmitted to an external controller and processed by an algorithm that measures cervical dilation. DiaCam's cervical diameter measurements are related to the mother/caregiver, providing quantitative indication of when active labor begins.

XZAMN

*Nicole Boyd, Michelle Feely, Aaron Maccabee, Xin Xiong, Zhener Zhang
Advisor: Prof. Qi Wang*

Diabetic foot ulcers (DFU) are open sores or wounds caused by tissue breakdown from restricted blood flow, lack of sensation, or trauma. Approximately 20% of the 30.3 million diabetes patients in the US develop a DFU in their lifetime. If DFUs are not detected and treated, they can progress to more severe, non-healing wounds that may eventually require amputation. The clinical standard for DFU detection and monitoring is a visual examination; however, there is not an in-home solution that provides comparable information about DFU location and size, which are critical parameters for wound tracking. XZAMN is an in-home use device that improves DFU monitoring via thermal and digital imaging, informing machine learning algorithms to localize and quantify the size of a developing DFU. The initial prototype testing indicates 80% sensitivity and 80% specificity for detection and localization of the ulcer, demonstrating that our device can provide quantitative, in-home monitoring of DFUs.

Stroke Alert

*James Gornet, Robin Guo, Minyong Jung, Destiny Machin, Lindsay Testa
Advisor: Prof. X. Edward Guo*

Stroke is one of the leading causes of death in U.S., with 795,000 cases annually and a 41% mortality rate. The current gold standard for stroke detection is through a bystander recognizing symptoms, such as facial drooping, arm weakness, and slurred speech, but accuracy is very low (38%), and a knowledgeable bystander is not always available. As such, 72% of patients reach a hospital outside of the treatment window for the most effective treatments. Therefore, there is a clear need for a reliable method to detect a stroke without the presence of a third-party. Stroke Alert provides a novel solution to this problem. Our wearable device detects hemiplegia, an early sign of stroke, by continuously monitoring blood pressure in the upper limbs. Contralateral reduction in blood pressure is an indicator of hemiplegia, triggering alerts from our system. The Stroke Alert monitor provides objective detection and does not require third-party monitoring. Initial testing shows that Stroke Alert can rapidly detect computer-simulated strokes, demonstrating its potential to provide a better alternative to the gold standard.

VisaVein

*Aubrianna Queen, Saiti Srabonti, Luke Thorsell, Zarmeen Mussa
Advisor: Prof. Barclay Morrison*

Venipuncture is the most common invasive medical procedure worldwide, yet nurses and phlebotomists often have difficulties locating the vein and inserting the needle correctly - particularly in pediatric patients who have poorly visible veins. Only 42.8% of pediatric needle insertions are successful on the first attempt. Incorrect insertions in children can lead to pain, nerve damage, and tissue necrosis. Existing assistive venipuncture devices often only provide 2-D information about vein location, leaving providers and patients susceptible to needle over insertion, a prevalent venipuncture failure mode. Our device proposes a two-pronged solution: vein visualization using tissue illumination and determination of successful insertion depth using a force transducer coupled to the needle. After initial testing, it was concluded that our device facilitates visualization of veins while the force feedback system provides critical depth information, providing comprehensive information for caregivers during needle insertion.

CEA Solution

*Maveric Abella, Emily Chen, Diana Lu, Lorenzo Talbot-Foote, Leah Zheng
Advisor: Prof. Clark Hung*

Postpartum hemorrhage (PPH) is the leading cause of maternal death in the world, with 99% of PPH-related mortalities occurring in low- and middle-income countries. Symptoms of PPH are difficult to distinguish during and after labor. Visual estimation of blood loss is the most practiced diagnostic technique, but this method requires continuous monitoring by healthcare personnel and fails to efficiently and successfully direct, collect, and quantify fluid, resulting in inaccurate estimations of blood loss. When hemorrhaging occurs, physicians must navigate diagnosis of PPH as quickly as possible to save patients' lives. Therefore, there exists a need for a device that can monitor and diagnose PPH in the critical 24 hour post-delivery period when mothers are particularly susceptible to PPH. The CEA solution facilitates accurate collection and quantification of blood loss, and alerts healthcare personnel to the onset of PPH.

CHEMICAL ENGINEERING

Natural Gas to Methanol Production Plant

Daniela Marin & Shirley Xu

Every day, about 200,000 tons of methanol are consumed. In 2015 the demand for methanol was 75 million metric tons and this demand for methanol has since been increasing. Due to the increasing demand of methanol, there have been a growing number of methanol plants across the world. Currently there are over 90 methanol plants. This growing methanol industry has brought in \$55 billion a year and created jobs for over 90,000 people around the world¹. Methanol production in North America is expected to increase by 26% by 2020, making the competition between methanol producers higher.² Because of this demand for methanol, many ways of producing methanol have been studied. One method of producing methanol is to make it from syngas. Since the methanol synthesis reaction is highly exothermic, it is important to understand the reaction kinetics and maintain control of each subunit to mitigate the possibility of a runaway reaction. Our team is presenting a bid for the construction of a \$1.26 billion additional component to an existing methanol plant. This design will produce 427,000 metric tons of methanol per year with a purity of 99.8% from 42.6 MMSCFD of natural gas. Of this natural gas, 26.4% will be used to produce 64.2 MW of net electricity. From sales of methanol and electricity, the plant gives an overall profit of \$281 million per year. The plant has a 99.6% methanol yield. The total depreciable capital and the total capital investment cost are \$1.098 billion and \$1.26 billion respectively. The profitability analysis concluded that the return on investment (ROI) is 17.6%, the payback period (PBP) is 3.5 years, the net present value (NPV) of the investment is \$497 million and the discounted cash flow rate of return (DCF RoR) was 21.9%.

¹ The Methanol Industry, <https://www.methanol.org/the-methanol-industry/>

² Morris, G. D. U.S. Methanol On The Comeback (2013). Retrieved December 10, 2018, from <https://www.aogr.com/web-exclusives/exclusive-story/u.s.-methanol-on-the-comeback>

CIVIL ENGINEERING

Fueled by the Elements: A Solar-Powered Resort

*Bailey Alexander, Samantha Grech, Tracy Paltoo, Carly Press, Abigail Thomas
Advisor: Tom Panayotidi*

This semester-long project aimed to design a solar-powered, locally oriented and socially conscious, storm-resilient resort on this northern coast of Puerto Rico in the Quebradillas region. Design of the 6-story eco-resort was approached from four civil engineering disciplines: Geotechnical Engineering, Structural Design, Environmental & Water Management, and Construction Management. The geotechnical engineering portion consisted of a literature-based analysis of the site's soil conditions and design of the foundation. Subsurface site conditions were assumed to be 5 meters of alluvium resting on limestone bedrock, for which a mat foundation was optimal. The mat foundation was analyzed using SAP2000. Structural design included dead, live, wind, rain, earthquake, and flood load calculations, from which the load bearing members were designed. These members were floor slabs, beams, girders, and columns. The structure was visualized in AutoCAD and analyzed using SAP2000. For critical members, the SAP2000 results were checked against hand calculations. Environmental considerations centered on solar energy and water reuse, incorporating LEED design concepts where ever possible. The minimum photovoltaic capacity and requisite solar cell infrastructure were calculated for solar power design. Stormwater routing analysis was performed for a 100-year, 1-hour storm to design the roof drainage and calculate more accurate rain loads, while a 1-year, 12-hour storm was used to plan the greywater recycling system. After design, project implementation was outlined by the construction management team. Overall costs were estimated and key construction methods, such as monolithic construction, were designated. Scheduling was laid out through a work breakdown schedule, network diagram, and Gantt Chart. The final result is an environmentally conscious, cast-in-place reinforced concrete building.

Keywords:

Design, engineering, geotechnical, structural, water, environmental, construction, SAP2000, solar-powered, resort, concrete, cast-in-place, monolithic construction, Puerto Rico, civil engineering, gray water recycling

The Prism

Salomon Dayan, Lorenzo Ferrari, Marco Della Genco, and Will Masters
Advisor: Tom Panayotidi

The Westside of the island of Manhattan is in the middle of a major redevelopment. With projects such as the Hudson Yards, The Spiral, the extension of the 7 line, and the retrofit of Penn Station, the Westside is becoming one of the most desirable places to live, work, and play in New York City. Although it might seem that most of the prime spots along the Westside have already been snatched up for redevelopment, there is still a large section of real estate along the Westside Highway between 45th street and 55th street that has yet to be capitalized upon. It is here, on a parking lot located at the corner of 45th street and the Westside Highway, we purpose building The Prism: a 46-story, 562 ft high, 616,000 sqft, LEED certified, all glass office building.

The Prism will be split up into four major parts. Starting from street level, the building will start out with a 150 by 105 foot lobby, containing 18-foot high ceilings and entrances to the 8 elevators and 2 staircases that service the building. The second section will be 15 stories high, each floor having the same floor area as the lobby, with 12-foot high ceilings. At the 17th floor, the building tapers in on the north-east and south-west corners, creating two 900 sqft terraces, both acting as greenroofs that will host native plants and give breathtaking views of the Hudson and Mid-town. The third section of The Prism will continue up with this new floor configuration another 15 floors until the 32th floor where the north-east and south-west corners are tapered in yet again, revealing four 900 sqft terraces. The next 15 floors continue with the same floor area as the 32nd floor until the 46th floor, topping off with a 10,350 sqft green roof, one of the largest in New York City.

The foundation of the Prism will consist of 357 steel-concrete composite pipe piles that will be drilled into the Manhattan Schist Bedrock located underneath the building. The piles will go directly into a 3.66 ft concrete pile cap which is designed to be built as one large concrete mat. The top of the pile cap will be the same elevation as the lobby, both sitting atop of 3 feet of compacted soil that will be brought in in order to make sure the entrance of the building would be safe in the event of flooding. There is no basement in The Prism, a design decision that was made in order to increase the building's resiliency to rising sea levels and more frequent super storms.

The Prism will be built entirely out of poured in place, reinforced concrete that will decrease in strength as the building increases in height. The core of The Prism is in the middle of the building, consisting of concrete shear walls that will transfer all of the lateral loads to the pile cap. Triple paned windows, filled with krypton gas and built in a steel frame, will line the entire façade of the building, enabling 360 degree views as well as a heightened level of thermal performance.

The Prism will be LEED certified (pending level of certification), which was achieved with design techniques such as green roofs, a gray water recycling system, highly efficient water and energy fixtures, bike and green vehicle parking, as well as the building's close proximity to public transportation and the Westside Highway Bike Path.

The cost estimate of the schedule is being conducted using the Unifomat framework. Using AACE International's Estimate Classification System, the estimate created for this project will be a level 2 estimate. The schedule was built using a bottom-up framework and checked with industry experts to obtain the highest level of predictability possible. The rental rates for the office spaces available are still being negotiated at this time.

Keywords:

Office buildings, Manhattan, LEED certification, green roofs, concrete structure, pile foundations, New York City, water recycling, building resiliency

New Cape Cod Bridge

Christopher DeFalco, Bryan Lei, Jessie Yan, Geyang Zhou
Advisor: Tom Panayotidi

The Cape Cod Canal separates the popular tourist destination, Cape Cod, from the rest of mainland Massachusetts. There are currently only two vehicular connections traversing the canal. The Sagamore and Bourne Bridges were both completed in 1935 for a 50-year design life, but are now over 80 years old. They are 45 and 40 feet wide, respectively, meaning that each bridge only has two lanes in each direction and no shoulders. There are 5.23 million visitors entering and leaving Cape Cod every year and the narrow bridges are struggling to cope with the heavy traffic that has descended upon this region over the last few decades. Traffic has been steadily increasing year-round; the combined off-peak daily traffic on these two bridges is 94,000 vehicles and jumps up to 136,000 vehicles, with backups up to 3.75 miles long during the summer peak season (MassDOT, 2014). The Massachusetts Department of Transportation is also worried that in event of a hurricane or some other natural disaster, terrible congestion and old bridges would pose a serious safety concern to the mass evacuation of the Cape.

We decided to focus on improving capacity on the Sagamore Bridge, because it carries 55% of the traffic, and its surrounding highways have been streamlined for better capacity. In addition, Route 6, the highway that connects to the Sagamore, traverses the entire Cape and carries more traffic than Route 28 connecting to the Bourne. We decided to build a twin-towered cable-stayed bridge directly west of the Sagamore, named the New Cape Cod Bridge. The towers of the bridge would be placed on land with a height of 387 feet, and a clearance of 135 feet below for marine traffic. The main span would be 1,024 feet, with an overall length of 1,800 feet. As outlined by MassDOT, the bridge would have three tolled lanes of on-Cape traffic, with the Sagamore converted to three off-Cape lanes that would not be tolled. There would also be a multi-modal lane for pedestrians and cyclists. With these guidelines, we decided on a 64 feet width, enough for a shoulder and the appropriate lanes.

Keywords: Cape Cod, Cable-stayed Bridge, Transportation, Infrastructure, Massachusetts Department of Transportation (MasDOT), Resiliency

Amazon's HQ2

*Isabel Neiva (team captain), Katherine Burt, Lin Ge, Min Hwang, Eleanor Rasbach
Advisor: Tom Panayotidi*

In September 2018, Amazon announced that they will build their next headquarters in Long Island City, Queens. Amazon plans to buy and develop four million-square feet of energy-efficient office space within 10 years, expanding to six to eight million-square feet within 15 years. This new campus will generate approximately 25,000 jobs and as a result the social, political, and economical dynamic of Long Island City will be forever altered. The campus must be designed such that it integrates with the existing community while meeting Amazon's criteria as a corporate giant at the forefront of technological innovation. For our project, we have designed a 540ft. high rise building to serve as office space for the new Amazon HQ2 campus.

We designed our structure in a way that follows new tech office layouts, ensuring the building has maximized the open floor plate, while minimizing the number of columns. Our building's structural system is made of up steel framing that supports the vertical loads acting on the building. The steel frame works with the reinforced concrete core system to take the horizontal loads, therefore transferring the moment to the concrete core. Our design also features a terrace system below the base of the building that serves to elevate the entrance of the building by 20ft in order to increase the building's flood resilience, as the campus is in a flood and storm-prone region of Long Island City.

Our building's substructure includes 3 floors of basement space, with each floor being 11ft. tall. The foundation begins 33 ft. below the first floor with a 2ft. thick concrete mat. This mat connects 660 15" diameter piles that reach the bedrock at a depth of 60ft. below the first floor. All of the piles are cast-in place reinforced concrete. The basement walls will employ waterproofing methods to protect the building from flooding.

The project will be delivered using the design-build method with a Guaranteed Maximum Price contract. Construction will begin in 2019 and be completed in 2022. Our estimated budget for this project is approximately \$1.2 billion. The project will use union labor and a General Project Plan to rezone the project site. All permits will be approved through the New York City Department of Buildings.

In order to contribute to the sustainability efforts of our project, our building will be LEED Gold certified. Access to quality transit, rainwater management, and indoor water use reduction are just some of the many items that earn us LEED points and make our building more environmentally friendly. We also are incorporating renewable energy and plan to wheel in solar power from nearby solar farms to lessen our carbon footprint.

Keywords: Amazon, office buildings, structural design, geotechnical design, water resources management, LEED certification, construction management, design-build, deep foundations, flood resilience, solar energy

San Francisco World Cup Stadium

*Carolina Garcia, Andrew Hathaway, DeWein Pelle, Rick (Yue) Yu, Yifan Zhou
Advisor: Tom Panayotidi*

Large infrastructure influences society by providing a platform to boost the economy. As the 2026 World Cup games approach, we are proposing to host the games in San Francisco by planning a monumental stadium. In honor of the coming 2026 World Cup, we chose to design and plan a stadium in San Francisco as one of several stadiums that can be used in the multi-nation hosting bid. The World Cup is an international spectacle that inspires awe in its billions of viewers and will inspire millions more to see it live. The 64 matches in the 2018 World Cup had a total live attendance of 3.43 million people and had 3.572 billion viewers worldwide —just under half of the world population (statista). Our team’s vision is to develop a proposal for a stadium located in Candlestick Point San Francisco, California that will do the World Cup a fraction of the justice it deserves.

The objective of this project is to develop an environmentally conscious and financially profitable multipurpose stadium with its first use intended for the 2026 World Cup. The structure itself will cover an area of approximately 800,000 square feet, not including the designated parking area. Our model has the capacity to hold over 70,000 people, which is more than enough to hold the average attendance of a 2018 World Cup match of 53,592 (statista). Work performed includes, but is not limited to, an analysis of the financial feasibility, the planning of construction, considering the potential market, and public transportation access to the stadium as well as the design of the stadium to optimize structural safety, integrity, and robustness of the structure and our implementation plan. The stadium design is executed using design tools known as SolidWorks and SAP2000 for structural and geotechnical engineering aspects, LEED standards for the environmental aspect, and Primavera for construction management. The structural design, modeled in SAP2000, features a concrete skeletal structure with seven floors and two tiers of seating bleachers, all of which rests upon a pile foundation. These seating bleachers and the roof system are both made of steel.

Once the World Cup has concluded, the stadium will service other markets to increase the financial viability of the venture. These markets would include a venue for concerts and other performances, non-World Cup soccer matches, and football games (as the fields are similarly dimensioned). The goal is to produce a stadium that the City of San Francisco and the nation can be proud of for generations to come.

Keywords: stadium, truss system, cable-stayed, LEED, steel, concrete, pile foundation, mat foundation, critical path method

EARTH AND ENVIRONMENTAL ENGINEERING

The Impact of Climate Change on Cities: Investigating the Urban Heat Island Effect in New York, Chicago, and Durban

*Priscilla Bell, Amit Krishnan, Eleni Reynolds, Nicole
Romola*

*Advisors: Dr. Christian V. Braneon, Goddard Inst. for
Space Studies and Robert Farrauto Professor of
Professional Practice*

As the world becomes increasingly urbanized, rising regional temperatures are experienced in expanding cities due to a phenomenon known as the Urban Heat Island (UHI) effect. Urban areas are prone to these UHIs as man-made construction materials facilitate rapid heat transfer and have different thermal conductivities than the natural environment. Additionally, densely packed buildings create a surface roughness that traps radiation and slows airflow, causing increased heating in urban air [1]. Water flow is also significantly altered in urban spaces, as cities are engineered to efficiently remove surface water from impervious surfaces. The evaporation rate decreases and a larger portion of radiation is instead utilized to heat the land surface and the above air [2].

Yuan and Bauer published a 2006 study detailing the effects of Normalized Difference Vegetation Index (NDVI) and percent impervious surface (eg. pavement, roads, industrial areas) as contributors to the UHI effect [3]. The results gathered in the study showed that land surface temperatures (LST) very strongly correlate with percent impervious surface. This was studied further by Liu and Zhang, who attempted to correlate LST with NDVI and found a correlation between “green”, well vegetated land and lower land surface temperatures [4].

LST was calculated for New York City, Chicago, and Durban using two methods for years 1988-2018. One day from a 100-hottest day range was analyzed for each year. Method 1 was adopted from the USGS website on Landsat data use [5]. Thermal bands from Landsat and constants from the metadata were used to calculate top of the atmosphere spectral radiance, L_{λ} , and sensor brightness temperature, T_{sensor} . Emissivity, ϵ , is derived from NDVI, calculated using from spectral bands. Lastly, L_{λ} , T_{sensor} , and ϵ were pulled together in a final LST calculation. Method 2 was adopted from Jiminez-Munoz et al [6]. The LST equation used the same three values calculated in Method 1 with the addition of atmospheric correction functions, Ψ_1 , Ψ_2 , and Ψ_3 . These functions were calculated using the total atmospheric water vapor content, w , which was gathered from the NOAA Reanalysis-1 dataset.

There were two maps created for each year, for each city. GIFs were produced using maps from all years to show the change in hotspot locations, defined as the top 10th percentile in temperature, over time. The LST maps from 1988-2018 for the analyzed cities were combined into

singular weighted sum visualizations, showing areas that are most frequently temperature hotspots (Figures 1-3). Large parks, such as Central Park in NYC and Lincoln Park in Chicago, and bodies of water such as Natal Bay in Durban all consistently registered LSTs in the bottom 10th percentile. Conversely, dense urban areas such as the Financial District, Brooklyn, Queens, and Harlem in New York, and Near West Side in Chicago registered as the hottest areas. This analysis shows the impact of the built environment on temperature hot spots.

References

- [1] de Faria Peres, Leonardo, et al., "The urban heat island in Rio de Janeiro, Brazil, in the last 30 years using remote sensing data." *International Journal of Applied Earth Observation and Geoinformation* 64 (2018): 104-116.
- [2] Imhoff, Marc L., et al., "Remote sensing of the urban heat island effect across biomes in the continental USA." *Remote sensing of environment* 114, no. 3 (2010): 504-513.
- [3] Yuan, Fei, and Marvin E. Bauer. "Comparison of impervious surface area and normalized difference vegetation index as indicators of surface urban heat island effects in Landsat imagery." *Remote Sensing of environment* 106, no. 3 (2007): 375-386.
- [4] Liu, Lin, and Yuanzhi Zhang. "Urban heat island analysis using the Landsat TM data and ASTER data: A case study in Hong Kong." *Remote Sensing* 3, no. 7 (2011): 1535-1552.
- [5] "Using the USGS Landsat Level-1 Data Product." *Landsat Missions Timeline | Landsat Missions*. Accessed November 29, 2018. <https://landsat.usgs.gov/using-usgs-landsat-8-product>.
- [6] Jiminez-Munoz, Juan C., et al., "Revision of the Single-Channel Algorithm for Land Surface Temperature Retrieval from Landsat Thermal-Infrared Data." *IEEE Transactions on Geoscience and Remote Sensing* 47, no. 1 (2009): 339-349.

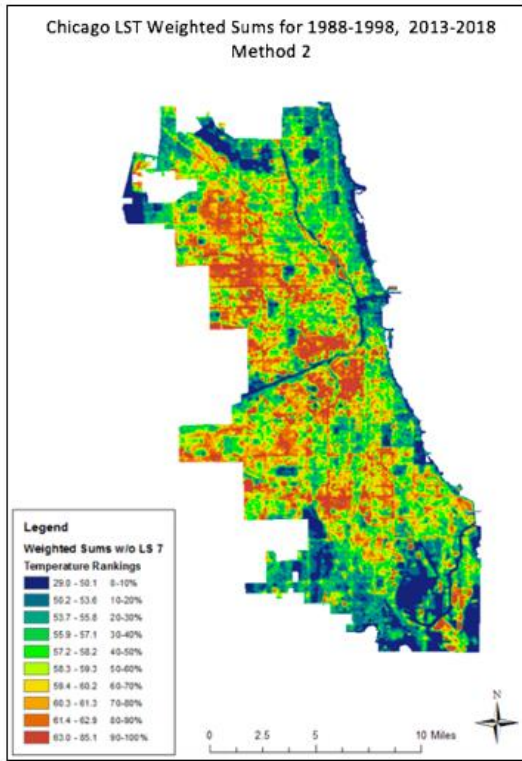


Figure 1: Chicago LST Weighted Sums Map

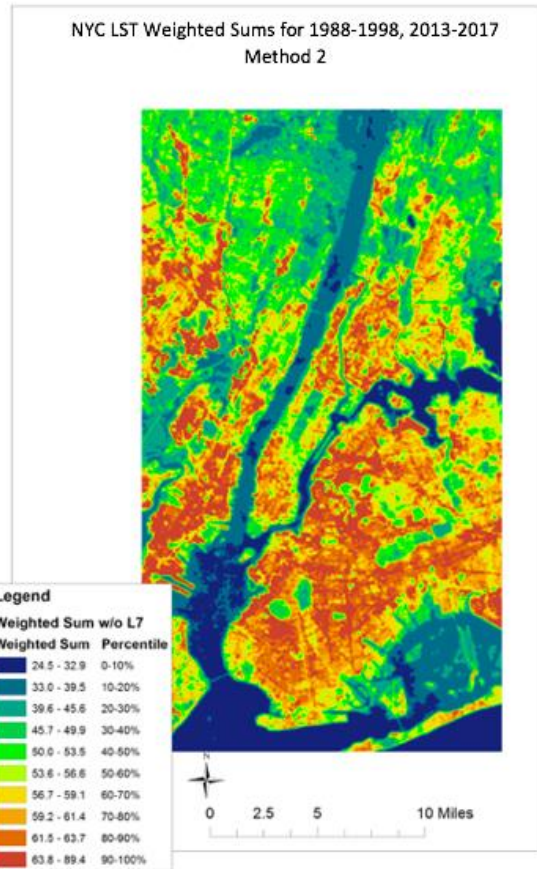


Figure 3: NYC LST Weighted Sums Map

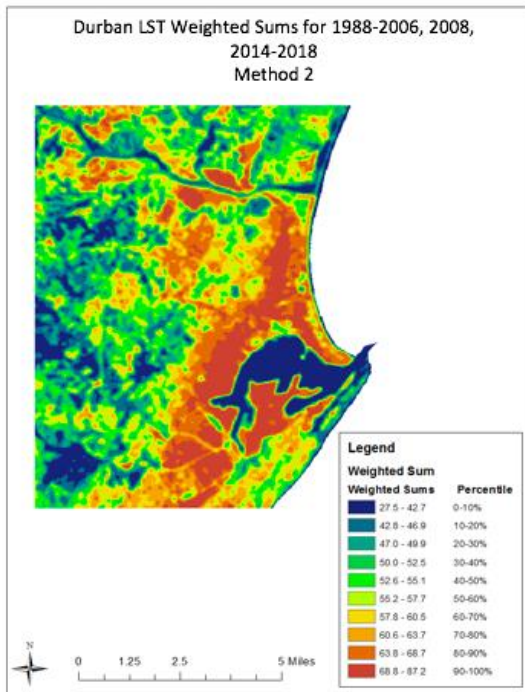


Figure 2: Durban LST Weighted Sums Map

Retrofitting Heating and Cooling Systems with Variable Refrigerant Flow System on Columbia University's Morningside Campus

Ji Ho Jeon, Iris Lin, Yueli Liang, Yukun Yang

Advisor: Robert Farrauto

Variable Refrigerant Flow (VRF) is an air-source heat pump (ASHP) technology that can be used to heat and cool spaces. ASHPs are high-efficiency electric appliances that transfer heat rather than generate it. Compared to conventional steam boiler system, ASHPs save energy, reduce greenhouse gas emissions, and greatly improve resident comfort, offering multifamily buildings a path to electrification.

This retrofit project aims to analyze the possibilities of implementing ASHP systems to McBain Hall, a residential building for Columbia undergraduate students. A number of different heat pump models are selected based on the building conditions and weather conditions of New York City. From assessing the energy consumption of the building, conducting an economic feasibility study of ASHPs, and calculating CO₂ emissions, a specific VRF system design will be suggested.

Calendar Year 2016-2018 electricity bills from Con Edison were used for the energy usage analysis. Electricity and natural gas consumption and demand profiles were used as the primary source to evaluate the capacities of selected ASHPs and estimated installation costs. Furthermore, environmental impact analysis was conducted to calculate CO₂ emissions reduction of converting heating source from natural gas to electricity.

OpenStudio 2.7.0 was used to run the ASHP simulation on EnergyPlus. The model was built using SketchUp Pro 2017 with the Legacy OpenStudio Plug-in. Local weather data, energy constructions, loads, space types, facility information, geometry, thermal zone, and HVAC systems were adjusted to match the real world conditions for this simulation.

The coefficient of performance varies from 2.05 to 3.20 for air source heat pumps based on different models and temperatures, and 1 for the steam heating system. Therefore, when the ambient temperature is at 47°F, by implementing the air source heat pump, the carbon dioxide emission will decrease by 54-69% or 475-602 kilograms; and when the ambient temperature is at 17°F, the carbon dioxide emission will decrease by 50.5-52.3% or 1187-1230 kilograms.

An electricity grid update would be needed before installing high capacity heat pumps on the rooftop of McBain. After the renovation, old radiators and conventional ACs would be replaced by multi-zone indoor unit connecting to heat pumps.

Acknowledgments

This work was supported in part by Columbia University's Department of Facilities and Operations. The authors thank Dominick Chirico, Tak Eng, and Robert Kishun for discussions and granting access to McBain Hall's utility data and floor plans. We also thank Noah B. Rauschkolb for his help with building energy simulation. Furthermore, the Energy Usage Analysis tool was provided by EN-POWER GROUP, an energy engineering firm located in New York City. We thank Amalia Cuadra, Sean Lee, and Griffin Teed for granting access to their tool and providing guidance in designing the VRF system.

**Water Reclamation and Salinity
Abatement: A feasibility survey to
implement potable reuse in Manalapan,
NJ**

*Zoë Berry, Ansley Carlisle, Rachel Lujan
Advisor: Professor Robert Farrauto*

Potable reuse, a process in which treated wastewater is reclaimed as drinking water either indirectly or directly, is gaining popularity as a sustainable and cost-effective solution to water resource depletion across the country and the world. In the northeast United States, winter weather typically raises salinity levels due to the spreading of road salt for de-icing roads. Currently, SUEZ Water, the owner and operator of the Manalapan Water Treatment Plant (WTP), intakes water from the nearby Matchaponix Brook as the drinking water source and supplements as needed from two aquifer withdrawal wells. The salinity of the Matchaponix Brook is regularly over the state water quality standard for dissolved salts, so blending with high-quality groundwater is necessary to dilute the salt content and meet the water demand from both the Manalapan and Freehold Townships. These withdrawals from the confined aquifer for potable use are causing significant decreases in the water level of the aquifer. A wastewater treatment plant, owned by Western Monmouth Utilities Authority, is located less than 1000 meters northeast of the Matchaponix WTP, and may be utilized as a potential source of water for indirect potable reuse (IPR). Three solutions were proposed to both reduce salinity in the drinking water and recharge the aquifers: IPR with reverse osmosis, IPR with electro dialysis reversal, and non-potable water reuse with no additional treatment. Cost-effectiveness analyses, design specifications, and social-environmental benefits were developed for each solution. Results show that adding

electrodialysis reversal to the wastewater treatment process is the most effective solution. As an alternative, it is recommended that SUEZ Water and Western Monmouth Utilities Authority keep the current wastewater treatment train and use the treated water for industrial and agricultural uses, thus increasing the amount of drinking-quality water available for potable use. It is also recommended that steps be taken to address the source of increased salinity, i.e. road salt, of the region's surface water.

Save the Trout! Framework for the Cold Water Releases in the Delaware River Watershed

*Rachel Barkowitz, Daniel Dray, Lillianne Farih,
Heather Morriss*

*Advisors: Professor Peter Kolesar and Professor
Robert Farrauto*

The Delaware River is a vital resource for the many people who depend on it. The river is a source of drinking water for almost 5 percent of the human population in the United States, including the entirety of New York City and Philadelphia¹. Due to its importance, the political differences between stakeholders can make decisions about water usage difficult to agree upon.

Delaware River trout are a cold-water species and are subject to the fluctuating temperatures of the river. As determined by the New York State Department of Environmental Conservation (NYDEC), the upper limit of the preferred temperature range for both brown and rainbow trout – the trout species common to the Delaware River – is 68°F (20°C)². If water temperatures exceed 75°F (23.9°C), Delaware trout enter periods of “severe thermal stress”³. Cold-water releases from dams on the Delaware River can help mitigate the high-water temperatures and therefore mitigate the thermal stress conditions for trout. As a preventative measure, 2,500 cfs-days’ of water has been allocated as a thermal mitigation bank to be used to prevent thermal stress events from occurring.

This project set out to accomplish the following main tasks: (1) determine the conditions that lead to thermal stress events at Lordville, a gauge downstream from one of the main dams in the Delaware; (2) create a linear-regression based statistical model to help predict when thermal stress events would occur at Lordville in the future; (3) create a decision dashboard for New York State DEC to implement in their daily decision making on whether or not to make a thermal release; (4) determine if the 2,500 cfs-days cold-water bank is sufficient to mitigate stress in Lordville during the summer season (May through September) of each year.

To accomplish the tasks outlined above, 78 days were identified as thermal stress days between

2008 and 2018 where the daily Lordville maximum water temperatures met or exceeded the benchmark of 75 degrees Fahrenheit. These 78 days were classified into 26 distinct thermal stress events. Data for climatic and river conditions on these days was used to determine what combination of conditions leads to stress events. It was found that a combination of high air temperature and low water discharge led to thermal stress events in Lordville. A linear regression model was created using discharge levels from several gages, water temperatures, and the actual/forecast air temperatures in Binghamton, NY. The 12-hour time delay between the cold-water release point and Lordville was considered when creating this regression model, and the model divided available data in half – one portion was used to fit the regression, and the other was used to measure the prediction potential of the regression. Using results from the model as well as known conditions, an interactive decision dashboard was created. This dashboard takes significant variables as inputs, and if enough conditions are met, informs the decision-maker that a thermal stress event is likely to occur at Lordville. The dashboard correctly predicted 64 out of 69 Lordville thermal stress days – 21/25 stress days and 23/26 nonstress days. Using both liberal and conservative estimates, the model predicted that the 2,500 cfs-days’ allotment was adequate to prevent any thermal stress events at Lordville in 8 of the past 11 years tested.

References

¹“The Delaware River -- A Little Known Natural Treasure,” Delaware Riverkeeper Network, 2018. [Online]. Available:

<http://www.delawariverkeeper.org/delaware-river>.

²K. Henson, "Mitigation of Thermal Stress in the Delaware Tailwaters: FFMP Performance and Proposed Guidelines for Mitigating Extraordinary Thermal Conditions," 2012.

³A. Ravindranath, N. Devineni, and P. Kolesar, "An environmental perspective on the water management policies of the Upper Delaware River Basin," *Water Policy*, wp2016166, 2016.

ELECTRICAL ENGINEERING

A Baseball Strike Zone Delineator Implemented Using Digital Image Processing Techniques

Joon Mo Park

Advisor: David Vallancourt

Contrary to the popularly held notion that the baseball strike zone is rectangular and is fixed, the strike zone is actually constantly changing as the batter is making movements to hit the baseball and has a shape of a pentagonal prism. The proposed delineator calculates for the position of the strike zone using input images obtained from the two set-up cameras and using digital image processing techniques. The delineator aims to aid the umpires in the process of determining whether a pitch is a strike or a ball by providing them an environment where they can compare their calls with those calculated from the algorithm. It should be noticed the main purpose of the proposed delineator is for the training of the umpires. Therefore, the batter wears red LEDs, that are used to track the batter's shoulders, top of the uniform pants, and the kneecap with the help of digital image processing techniques.

There exist three main objectives for the implementation of the strike zone delineator: the detection of the baseball, the home plate, and the batter's body. The detection of the baseball is achieved using the idea that the baseball is circular and white. Therefore, an algorithm that looks for round objects in an image was developed in order to successfully detect the baseball. After the conversion of rgb input images to grayscale images, binarization was

implemented, and the metric that indicates the roundness of objects was calculated. The binarization is essential in the implementation of the delineator since it enables the detection of the home plate. The binarization of images detects boundaries of different objects in an image, and it is for certain that one of the objects detected is the home plate of interest. The only problem now is to figure out which detected object is the home plate. The Speeded-Up Robust Features (SURF) algorithm was implemented in the process of filtering out detected objects that are not the home plate. Matlab's object recognition using SURF is composed of three steps: feature extraction, feature description, and feature matching. In other words, the SURF algorithm enables the detection of an object that is similar to an inputted reference image, which in this case would be the home plate. The last objective is the detection of the batter's body. More specifically, the batter's shoulders, top of the uniform pants, and the kneecap must be all detected in order to calculate for the strike zone. The batter would wear red LEDs for the implementation of the red segment filtering algorithm. The idea of the red segment filtering algorithm is that all pixels of the rgb images have values for their red, green, and blue components. The algorithm subtracts the grayscale values of images from those containing only the images' red components.

References

1) Gonzalez, R. and Woods, R. (n.d.). *Digital image processing*. 2nd ed. Prentice Hall.

2) Mathworks.com. (2019). *Identifying Round Objects- MATLAB & Simulink Example*. [online] Available at: <https://www.mathworks.com/help/images/identifying-round-objects.html> [Accessed 25 Apr. 2019].

3) Mathworks.com. (2019). *Object Detection in a Cluttered Scene Using Point Feature Matching- MATLAB & Simulink*. [online] Available at: <https://www.mathworks.com/help/vision/examples/object-detection-in-a-cluttered-scene-using-point-feature-matching.html> [Accessed 25 Apr. 2019]. 4) Nasir, S. (2019). *Color Detection in Images using MATLAB - The Engineering Projects*. [online] The Engineering Projects. Available at: <https://www.theengineeringprojects.com/2015/11/color-detection-in-images-using-matlab.html> [Accessed 25 Apr. 2019].

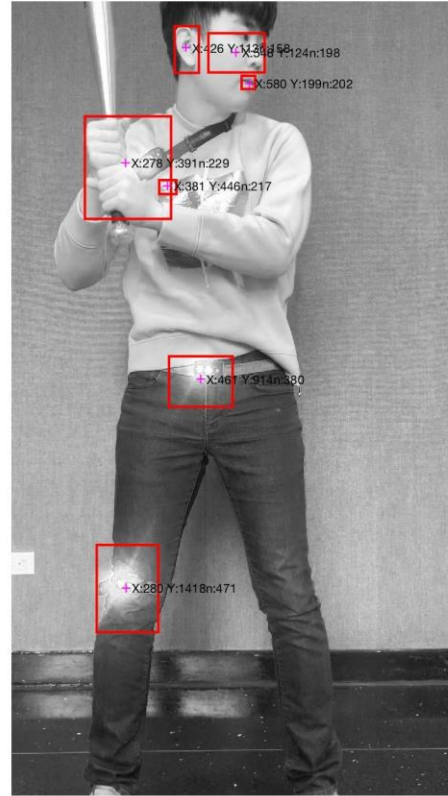


Figure 2: Camera facing the batter



Figure 1: Camera behind the batter

Dual-Axis Interactive Base

Chris Bhim, Marielle Jones, Luis Perez,
Neel Singal
Advisor: Dr. David Vallancourt

We commenced our project by fabricating a dual-axis solar tracker. The fabricated solar tracker can be seen below in figure 1.¹ Subsequently, the solar tracker was modified to be able to tilt accordingly, allow a dropped ball to hit the surface, and hit a moving target.

We removed the solar cell and the photodiodes but kept the Arduino shield that allowed us to control the two 9g servos. We also cut and placed a layer of plexi glass on the surface of the dual axis base. The plexi glass allowed us to elastically bounce balls off of the surface. As shown in figure 2, one servo allowed us to control the horizontal rotation of our base while the second servo controlled the vertical rotation. These angles could be acutely tuned using a microcontroller and corresponding shield. We determined the optimal vertical rotation angle through trial and error. Using a camera and OpenCV on python, we were able to track the trajectory of a moving target circling our base and determine the appropriate angle of horizontal rotation.²

To simplify our calculations, we ensured that the ball was being dropped from a predetermined height to allow for a constant acceleration and hence consistent collision velocity. To achieve this, we build a scaffold over our base. We then used a cylindrical funnel attached to a piece of plywood with a circular hole drilled into it. Subsequently, we placed a cylindrical funnel underneath the hole to ensure that the ball would have a consistent trajectory (refer to figure 3). Additionally, we developed some interactive, carnival-like games.

References

- [1] Zimmerman, J. (2017). Dual Axis "Smart" Solar Tracker 2.0. BrownDogGadgets. Retrieved April 9, 2019, from <https://browndoggadgets.dozuki.com/Guide/Dual-Axis-Solar-Tracker-2.0/14>.
- [2] Rosebrock, A. (2015). Ball Tracking with OpenCV. Pyimagesearch. Retrieved April 9, 2019, from <https://www.pyimagesearch.com/2015/09/14/ball-tracking-with-opencv/>.
- [3] Frazier, G., Taddiken, A., Seabaugh, A., & Randall, J. (1993). Nanoelectronic Circuits Using Resonant Tunneling Transistors and Diodes. Texas Instruments Inc.

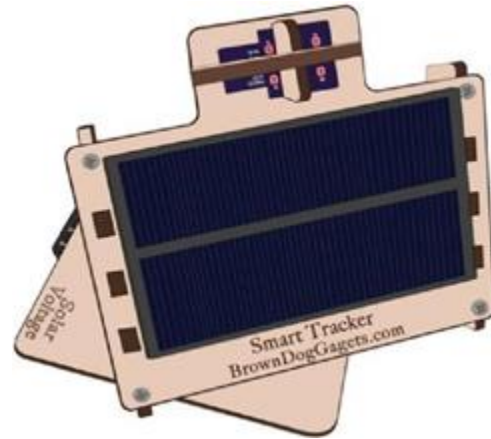


Figure 1: Fabrication Dual-Axis Solar Tracker from BrownDogGadgets



Figure 2: Base with 2 axes of rotation using two 9g servos

Frequency Stabilization and External Control Module for the Buchla 100 Analog Music Synthesizer

William Mauro

Advisor: Prof. David Vallancourt

Analog oscillators have long been plagued by frequency drift due to temperature effects and component parameters which vary with age, especially in the case of discrete designs. Such oscillators find common use as a sound source in electronic music synthesizers like the historic Buchla 100 modular system, however the inherent susceptibility of analog oscillators to frequency drift necessitates constant retuning which interferes with studio recordings and live performance alike. Frequency stabilization techniques are routinely employed to synchronize oscillators in communication systems but as of yet have seldom been adapted for use in musical circuits.

The Frequency Stabilization and External Control Module offers a novel pitch stabilization solution for existing electronic music synthesizers while also providing facilities for external control by a special purpose keyboard and the MIDI standard.[1] Eight identical stabilization channels are offered to the user which may be engaged simultaneously in order to allow for polyphonic control. The module operates by constantly measuring the frequency of a musical tone oscillator in the Buchla 100 synthesizer and continually adjusting its tuning control voltage to maintain a constant output frequency. Frequency measurement is accomplished using an embedded system based on the high-performance STMicroelectronics Arm Cortex-M7 32-bit RISC core for extremely precise readings to within 0.1 Hz.[2] Measurements are rapidly obtained by counting the number of clock cycles during a single period of the input signal from the analog oscillator. The measurement is compared with a desired frequency selected by the user and the resultant difference dictates the amount of control voltage offset necessary to keep the analog oscillator locked in tune. In order to produce the tuning control voltage output, the microprocessor is

connected over an SPI bus to an AD5360 16-bit digital-to-analog (DAC) converter which provides extraordinary accuracy theoretically to within 1mV.

The Frequency Stabilization and External Control Module provides several modes by which the user is able to choose the stable pitch frequency for the analog oscillator. "Keyboard" mode allows the user to select the pitch frequency in a conventional manner by actuating piano keys on a special purpose-built keyboard in either monophonic (single-note), polyphonic (multiple-note), or split configurations. Additionally, the tone interval between notes on the keyboard can be varied using a potentiometer mounted on the panel in order to allow for playback of non-western musical scales. A bar strip of indicator lights displays the channel configuration of the depressed keys. Furthermore, an implemented joystick controller mounted next to the keyboard may be used to alter several tone characteristics. The "MIDI" and "MIDI CC" modes allow the analog oscillators of the Buchla 100 to stabilize at frequencies dictated by MIDI note or continuous controller (CC) information from a computer or external device. MIDI data is received on the UART channels of the STM32 embedded microcontroller. The MIDI standard is widely adopted in modern electronic musical instruments and computer interfaces, allowing for an extensive variety of control options.

References:

[1] *The Complete MIDI 1.0 Detailed Specification.* [Online].

Available:

<https://www.midi.org/specifications-old/item/the-midi-1-0-specification>.

[2] STMicroelectronics, "32-bit Arm® Cortex®- M7 400MHz MCUs," STM32H7 Datasheet, Jun. 2017 [Revised Jul. 2018]

Chaotic DJ

Ryan Arteaga, Jinglei Guo, Ishraq
Khandaker, Hongyi Li

Advisor: Professor David Vallancourt

The Chua's Circuit, as shown in Figure 1, is a circuit that is capable of producing chaotic oscillation behavior. It consists of five elements: a resistor, two capacitors, an inductor, and a Chua's diode (a negative resistor). The Chua's diode can be implemented with two operational amplifiers with positive feedback and six resistors, connected in the system shown in Figure 2. The inductor in the circuit can be replaced with a gyrator to obtain a "simulated inductor" as shown in Figure 3. The Chua's Circuit has many applications. It can be used as a physical source of pseudo random signals and use synchronization studies regarding communications systems [1].

The purpose of this Senior Design Project is to explore the Chua's Circuit design and its effects on musical signals. Since the Chua's Circuit has a chaotic oscillating output (Figure 6), it can be used to create a random effect on musical input source. To achieve this musical effect, the chaotic output of the Chua's Circuit is sent into an Arduino Uno microcontroller. The microcontroller controls a stepper motor in response to the chaos from the Chua's Circuit and changes the potentiometer of a Dunlop Cry Baby Wah Pedal. A music source is plugged into the pedal and a random effect is added by the motor-controlled potentiometer to produce an output with a random wah effect.

The Chua's Circuit designed for this project produced an output voltage of 5 Vp-p with a dominant frequency around 300 Hz. The microcontroller for this design, however, can only take positive voltages through the analog input channels. Thus, the output of the

Chua's circuit is sent through a bypass capacitor and a bias resistor, to create a DC offset of oscillation signal.

The microcontroller processes the analog input from the Chua's Circuit and records the number of zero crossings. For every 1000 counts, it will trigger the step motor for 200 steps and thus control the potentiometer of the wah pedal. The motor will then reset the potentiometer back to the original position and restart the count for the zero crossings.

In conclusion, after careful analysis and extensive simulations, the chaotic behavior of Chua's Circuit is successfully achieved and applied into a musical system to produce audible results with random wah effects.

References

- [1] L. O. Chua, "Chua circuit," *Scholarpedia*. [Online]. Available: http://www.scholarpedia.org/article/Chua_circuit. [Accessed: 4-Apr-2019].
- [2] "Components for building Chua's circuit," *www.chuacircuits.com*. [Online]. Available: <http://www.chuacircuits.com/howtobuild2.php>. [Accessed: 4-Apr-2019].
- [3] "How to build Chua's circuit," *www.chuacircuits.com*. [Online]. Available: <http://www.chuacircuits.com/howtobuild1.php>. [Accessed: 4-Apr-2019].

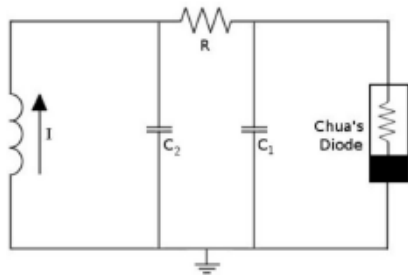


Figure 1: Chua's Circuit Schematic

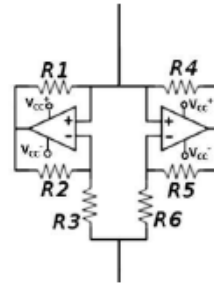


Figure 2: Chua's Diode Schematic

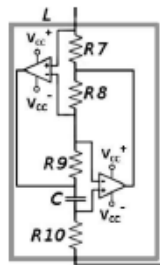


Figure 3: Gyrator Schematic

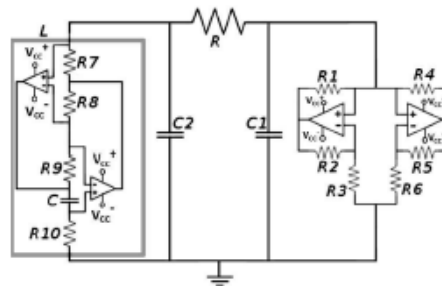


Figure 4: Chua's Circuit Complete Schematic

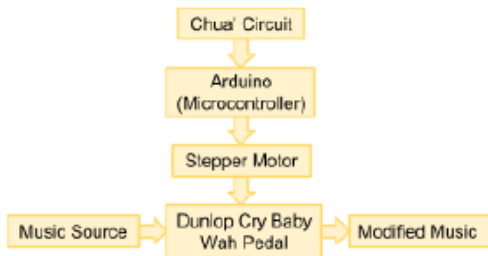


Figure 5: System Block Diagram

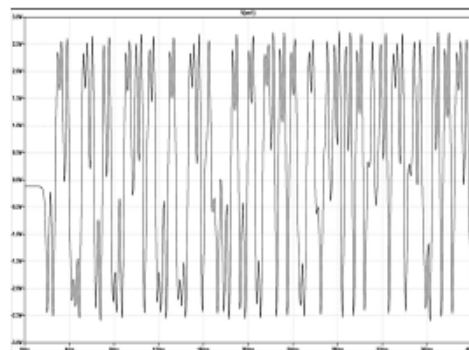


Figure 6: Chua's Circuit Output

Homemade Single-Supply Class D Amplifier w/ Bluetooth

Jay Mok & Chase Stine

In this project, we made a class D (A.K.A. PWM) amplifier. The class D amplifier offers lower power dissipation than other classes (A, B, AB) [5]. The reason is because the transistors are used as ideally lossless switches *rather* than as linear amplifiers.

The input audio signal is amplified as follows: the input goes into a pre-amplifier for filtering and small signal amplification. Then, it is compared with a triangle wave and transformed into two copies of itself: the

PWM signal and its inverse (i.e. phase shift of 180, negative of itself). The two PWM signals then are fed into a gate driver IC, which is able to turn MOSFET switches arranged in full-bridge configuration quickly. The amplified PWM signal is then low pass-filtered via lossless elements (L and C) and some other filtering configurations (snubbers). The speaker (subwoofer/mid-range in our case) is then connected as a bridge-tied load across the full-bridge switching amplification stage. This is a conventional design for full-bridge class-D amplifiers [2]. We choose to build the amplifier from scratch out of discrete components, like in previous DIY projects [3, 4] rather than use an IC, which is what is usually done for commercial designs [6].

The Class-D amplifier is also powered by a single-supply rather than dual-supplies as found often. Thus a positive power supply unit is also built from scratch. The design of the PSU is largely based on a previous design of a 10A unregulated power supply [7]. The major difference is the use of un-regulated supply rather than regulated supply based on recommendations from a book on audio amplifiers [8].

Originally we designed in amp feedback based on ideas from an old paper about amplifiers but due to stability issues, and severe time constraints, we decided to just use a non-feedback open-loop amplifier [1]. However, if given more time, we would have liked to include amplifier feedback.

We use a bluetooth receiver 2 audio jack module, rather than build the bluetooth from scratch.

We also use common IC and components found in university electronic laboratories, making this project not too difficult to implement. Furthermore, this capstone project combines knowledge from analog/digital electronic circuits, power electronics, signals and systems (filters), solid state (transistors), heat transfer (heat sinks), and electronic layout, making for a great chance to use what was learned in an undergrad EE curriculum.

References

- 1.Slobodan Cuk and Robert Erickson, "A Conceptually New High-Frequency Switched-Mode Amplifier Technique Eliminates Current Ripple," Powercon 5, pp. G3.1-G3.22, May 1978.
- 2.Simon Tonnarelli, "100W Class D Amplifier", Simon's Satcom Page , April 2017
<http://satcom.tonnarelli.com/ClassD.htm>
- 3.GreatScottLab, "DIY Class D Audio Amplifier", Instructables , 2018
<https://www.instructables.com/id/DIY-Class-D-Audio-Amplifier/>
- 4.Cezar Chirila, "How to Build A Class-D Power Amp", AllAboutCircuits , August 2016
<https://www.allaboutcircuits.com/projects/how-to-build-a-class-d-power-amplifier/>
- 5.Gaalas, Eric. "Class D Audio Amplifiers: What, Why, and How.", Analog Devices , June 2006, www.analog.com/en/analogdialogue/articles/class-d-audioamplifiers.html.
- 6.NXP, "TDA8954 2 × 210 W class-D poweramplifier", NXP Datasheet, December 24 2009, <https://www.nxp.com/docs/en/datasheet/TDA8954.pdf>
- 7.Vazerick, "Design and Implementation of a 10 Amp Linear Power Supply", Instructables , 2016
<https://www.instructables.com/id/10Amp-Linear-Power-Supply/>
- 8.Douglas, Self. "Audio Power Amplifier Design Handbook", Newnes, 1996

Semi-Parametric Equalizer using 20 Bands for Creating Arbitrary Frequency Responses

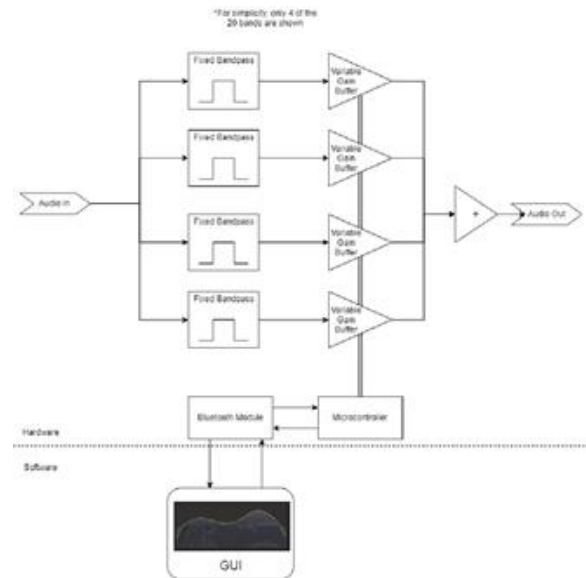
Jose Rubianes
Advisor: David Vallancourt

Many analog equalizers have only 3 bands, and offer relatively crude control over their frequency response. If one wanted to have finer-grained control over real-time audio, their current options are limited to large rack-mounted DSP units, expensive parametric equalizers tailored for professional applications, or software plugins. There is a current lack of affordable options for prosumers who want finer-grained control over real-time audio. The goal of this project was to create a small and relatively inexpensive semi-parametric equalizer to fill this niche.

The QWit allows the user to program nearly any arbitrary frequency response. Despite being digitally programmable, all equalization is done using analog filters, avoiding the delay associated with digital signal processing.

This is accomplished by using 20 second-order bandpass filters, where the gain of each filter is controlled by digitally-programmable potentiometers. Due to the large number of bands, the ability to control the gain of each allows the user to closely approximate almost any frequency response. Furthermore, the large number of bands negates the need for programmable Q control, which would have been expensive to implement.

The user is able to create the desired frequency response via the GUI on their computer or smartphone, which then computes the necessary band gains and sends the required potentiometer settings to the on board micro-controller. These settings are saved in EPROM, so that they can be automatically restored in the case of a power cycle.



Logic Board

*Leah Feuerman, Jacqueline Napolitano,
Sayaan Nawaz, Jackson Welles
Advisor: Professor David Vallancourt*

We are coordinating with Columbia Secondary School to develop an educational game to teach students the fundamentals of computer hardware and logic. We hope to do this in a more engaging and visual way than is done in typical college courses, so to be able to present the material to a younger age group and spark an interest in engineering early on. Our project will involve allowing student to build their own logic statements using their hands, and see the results with both a computer interface and the structures they build.

Using physical electronic logic blocks, we will allow students to discover the principles of Boolean algebra as performed on binary signals. Each interconnecting block contains a simple circuit to define their functionality. Individual blocks will include AND, OR, and INVERT gates, INPUT and OUTPUT variable blocks, TIMER and binary COUNTER circuits, as well as a POWER supply block. Each block will also contain a multicolored LED light, which will present the student with real-time information on the connections and information received and sent by the blocks.

A graphic user interface (GUI) will present the students with logic prompts and allow them to define the INPUT blocks based on

the riddle they are solving. As the students attach the INPUT blocks to other gate blocks in order to solve the riddle, the GUI will dynamically generate a graphic representation of what the students are building -- in short, as the students add blocks to their existing circuit assembly, the GUI will present the student with the connections that they are making, and can provide feedback to aid the student in solving the riddle.

Our curriculum will present various logic statements, an example of which can be found below:

Plant will grow if there is water and there is sunlight

There is sunlight but no water

There is no sunlight and no water

There is both sunlight and water

These simple statements will provide a blueprint to design the circuit using the logic blocks, and will include various parameters for the student to make modifications and further understand the functionality of the logic blocks.

The goal is to use a combination of challenging riddles, lights, and physical interactions with each component to develop a young student's fundamental understanding of how logic gates communicate. This will allow teachers and parents to present the foundations of electrical, computer, and software engineering to young students in a way that is both entertaining and interactive.

Modular Micropower Electronics for Fully Integrated Energy Storage Compatible with a Variety of Storage Media

*Peter Frey, Johnny Li, Michael Harriss, Max Möller
Advisor: David Vallancourt*

As energy storage and grid management become an ever more pressing issue in the world, new energy storage technologies have naturally become the topic of research interest. Many of these technologies require accompanying electronics in order to function as practical power sources, the specifics of which vary based on a number of factors related to their design. In this project we explore a possible design for a modular solution to accessing these alternative energy storage technologies, including DC/AC conversion of the output as well as charging capabilities, which can be scaled to power higher power devices [1]. Slight modifications on this design would allow it to be compatible with a wide range of contemporary energy storage devices, allowing users to easily adapt it to the specifics of their storage system.

Fundamentally, we need to design electronics to convert the DC voltage produced by the battery into stable 60Hz AC at 120V. When the energy storage system is in discharging mode, the DC voltage is supplied to the optocoupler and the H-bridge power inverter attached to a transformer. An Arduino using pulse-width modulation with frequency of 25kHz with a maximum of 50% duty cycle was used to control gate switching in order to achieve a simulated 60Hz sinusoidal output. An optocoupler is used to isolate the Arduino output and to supply the proper amount of current to the NMOS gates. Optimization of output power is achieved via fine-tuning of the supply voltage for the optocoupler and the NMOS. This output is then filtered and stepped up with a transformer to 115-120V ready to be attached to a load.

When the battery is switched to charging mode, the H-bridge portion would be disconnected from the transformer and the power supply would be disconnected from the energy storage to prevent leakage. The circuit takes in standard 60Hz AC which

is stepped down through the same transformer then converted to DC using a full-wave rectifier. The DC is then supplied as input to a Buck-Boost Converter in order to ensure a consistent charging voltage in accordance with the battery charging voltage. The duty cycle of the Buck-Boost converter is again controlled by the Arduino which takes voltage measurements as feedback to ensure the correct supply voltage is produced.

Lastly, we included functionality in the Arduino codes allowing it to take an external sinusoid as input and match the phase and frequency of the system output by altering the PWM and the voltage supply to the system. This allows multiple different storage solutions to be connected in parallel at the output side, reducing the cost of the system by limiting each individual units' current and making the project highly scalable and integratable towards high power application.

To test the circuitry we plan to use commercially available 18650 Li-Ion cells and build an iron chloride hybrid flow battery using graphite electrodes and a membrane of filter paper treated with sodium polyacrylate [2]. The flow battery serves as a good example of an energy storage solution which is promising in terms of environmental sustainability, life cycle, and ease of transportation, but which also requires significant accompanying circuitry in order to function as a practical power source, while the Li-Ion battery demonstrates the system's adaptability to market technologies.

References

- [1] Scholten, N. Ertugrul and W. L. Soong, "Micro-inverters in small scale PV systems: A review and future directions," 2013 Australasian Universities Power Engineering Conference (AU-PEC), Hobart, TAS, 2013, pp. 1-6.
- [2] Manohar, A., Kim, K., Plichta, E., Hendrickson, M., Rawlings, S. and Narayanan, S. (2015). A High Efficiency Iron-Chloride Redox Flow Battery for Large-Scale Energy Storage. *Journal of The Electrochemical Society*, 163(1), pp.A5118-A5125.

Pet-Minder: RFID Monitoring within Automated Food, Water, and Door Modules

*Benjamin Brigman, Asher Goldfinger, Anthony Gutierrez, Moises Peña
Advisor: David Vallancourt*

The idea for Pet-Minder is to create a system of modules that can identify a pet in a multiple pet environment, attributing a particular diet, monitor movements, and relay information about each one to a phone application. This is achieved by the construction of automated food and water dispenser and a “doggy-door” module alongside RFID tag communication multiple microcontrollers. Below includes explanations of each component of the design project.

RFID, Pet Identification:

RFID, or Radio Frequency Identification, technology comprises of a digital label that is transmitted by means of a range of radio wave frequencies. Much like a barcode scanner, the typical usage of RFID is based in inventory tracking or iD security, such as the locking mechanism in student dormitory doors.

The RFID system we are using requires a UHF, or Ultra High Frequency, reader module. For this design, an Arduino device is utilized as the reading mechanism for the sensor and the identification data is used across the system as a whole.

Each individual pet would have a collar outfitted with a n RFID tag, where a long-range UHF RFID antenna would be able to detect and identify a n animal 10 -15 feet from the base module.

Once a pet is identified, the automated modules are able to track the movement and health of the animal.

Diet Implementation:

Diet monitoring is regulated through automated food and water modules. Food regulation is predetermined by setting the amount and time of day for each mealtime. It is then dispensed at a given time and the bowl is moved out of the device when the RFID sensor finds a dog with a 10 ft radius of the device. The water module is programmed to continually have water available.

Weight scales are implemented in both devices to monitor food and water consumption, which is then transferred to the phone application. Monitoring which pet is eating or drinking at any time is done using a combination of data from movement sensors and the RFID scanner.

A food cover is included to discourage consumption from a pet that was not recognized for the mealtime as well. For example, if one dog has consumed all their food for the day, if they are with 10 feet of the device the food will be retracted into the device.

Pet Movement:

An electronic pet door is implemented to monitor pet movement in and out of the house, while also allowing the owner to lock the door in either, or both, directions. This is done through multiple linear actuators that place a bar to block the pet door’s pathway, locking the door to any traversing animal.

Each dog collar is equipped with a radio that listens on an interrupt for a certain frequency. The door is constantly sending a signal on this frequency directionally to outside the house. If the radio gets a response, meaning a dog is outside, the door will unlock from the outside. Otherwise the door will only be unlocked from the inside. The owner has manual control through the phone application of the indoor lock, limiting when their pets can go outside.

Smart Walker and Boot

*Mohammad Khojah, Shamirah Tillman, and
Ryan Davies
Advisor: David Vallancourt*

Falling is a serious threat to the health of senior citizens and people experiencing disability. On top of the fear that precludes them taking part in many activities, there are over 800,000 hospitalizations and 27,000 deaths each year attributed to falls. This explains the ubiquity of walkers, canes, and other devices in society as they increase the mobility as well as safety of those using them. However, these have their own problems and there are still around 47,000 cases of hospitalization each year from the improper use of them. It is with these issues in mind that our project aims to create smarter walking devices.

By combining embedded system and IoT elements with devices designed to assist mobility, we are able to add two levels of functionality. The first being feedback on how the patient is using the device and the second being emergency fall detection. The feedback can be split into real-time feedback delivered to the user via the device and data that is uploaded with the aim of being analysed later. The devices chosen to implement this smart design on were a two wheeled walker and a fracture boot.

Recovery requires that the injured area is still used to a certain extent to ensure that atrophy doesn't occur. At the same time, it is important to avoid overuse and failing to find that balance will increase the time it takes to recover. By measuring the weight the user puts on each device we are able to track whether they are putting too much or too little (through use of piezoelectric and gauge

sensors) and provide real-time feedback in the form of LEDs or buzzers. The thresholds of use would be preprogrammed onto the device by their physician or medical professional. The data generated through use is also available online so that the physician can check that the patient is following the prescribed regimen. This is accomplished by using the ESP8266 Wi-Fi module to upload data as the user generates it. Furthermore, by placing three sensors in the fracture boot it is possible to analyse exactly how the patient distributes their weight which may help identify unhealthy patterns of walking. Similarly, accelerometers allow us to track the three-dimensional gait which would also have specified thresholds that would need to be monitored and corrected when exceeded.

On the walker, accelerometers provide emergency detection through monitoring both tilt and acceleration. This is especially useful on the walker platform because in a majority of cases it is used by the elderly who require this safety feature.

This project aims to improve the quality of recovery through instantaneous feedback as well as a more informed physician and to improve safety through being able to alert caregivers as to when there may be an issue. Both of these functions assist the walker and fracture boot in their original aim improving the mobility of their user.

References

Stevens J. PhD, Thomas K. PhD, Leesia Teh ABJ, Greenspan A. PhD, "Unintentional Fall Injuries Associated with Walkers and Canes in Older Adults Treated in U.S. Emergency Departments", *Journal of the American Geriatrics Society*, 29 July 2009

The AWG short-reach (1<km) optical link

Runjia (Luna) Zhang

*Advisors: Prof. Keren Bergman and Prof.
David Vallancourt*

With the arrival of new technology, 5G for example, we are enabled with faster data speeds. For such computing speeds, we need optical communication systems. They use high carrier frequency of the electromagnetic spectrum. Fiber-optical communication systems are lightwave systems that use optical fibers for information transmission. During the evolution of both coaxial and microwave systems, one drawback of a high-speed systems is the relatively expensive operational cost. With optical waves used as the carrier, people have been able to increase the product of bit rate (B) and repeater spacing (L) significantly [1].

Silicon photonics, with silicon as an optical medium, allows higher transmission speed, less power consumption, and easily manufactured at the same mass scale as current silicon based technology. The progress in the development of silicon photonics technology foretells a future where optical interconnections replace the electrical wires over short distances [2]. In the near future, the primary application is expected to be cloud-based data center and potential application can be connected cars.

The AWG short-reach (1<km) optical link to be designed is shown as in the block diagram in Figure 2. Both fiber access networks and intra-datacenter networks (DCNs) can utilize such links. The link includes the PC, Arbitrary Waveform Generator (AWG), Electrical to Optical Converter (EOC), silicon photonics chips, Optical to Electrical Converter (OEC) and Real Time Oscilloscope (RTS). AWG generates electrical signals of PRBS source,

then each is modulated to optical signal using laser. The laser provides each signal with a specific wavelength. Then through multiplexer, those multiple channels of optical signals are transmitted over a single optical fiber using different wavelengths of light. The SiP chip contains multiple ring filters which together act as a demultiplexer. Each optical signal is converted back to electrical using O/E converter, and then sent to RTS, in order to compare with the original bit sequence and get the bit-error rate performance.

Acknowledgements

The author sincerely thanks Dr. Yanir London and Dr. Sasha Gazman for constant discussions, supports and insights.

References:

- [1] Govind, Agrawal., *Fiber-Optic Communication Systems* 1992.
- [2] Meisam, Bahadori., *Physical Layer Modeling and Optimization of Silicon Photonic Interconnection Networks* 2018
- [3] Mai, Thuy., Mai, T. (Ed.). (2017, August 07). *Benefits of Optical Communications*. Retrieved from https://www.nasa.gov/directorates/heo/scan/e_engineering/technology

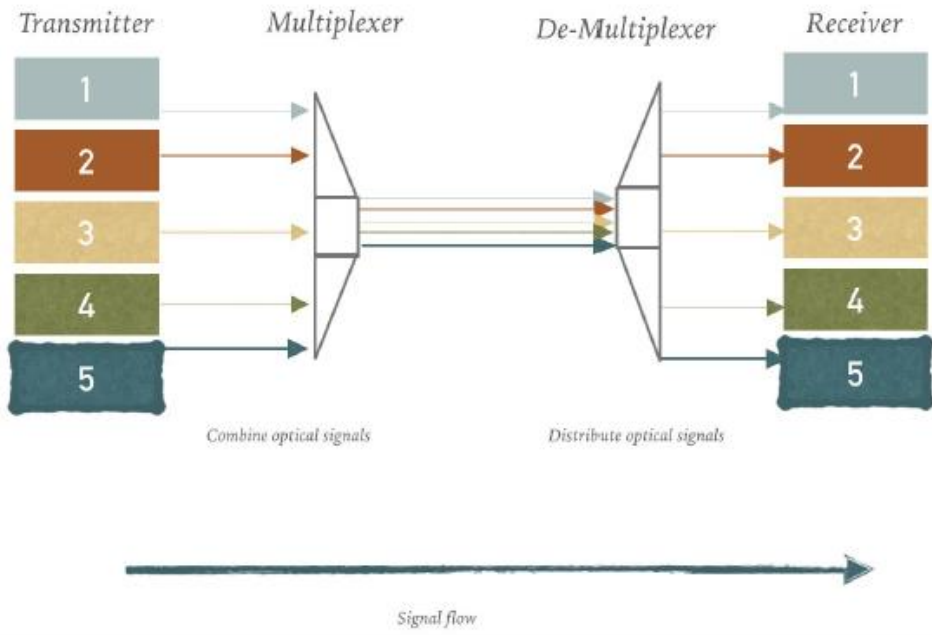


Figure 1: Wavelength Division Multiplexing (WDM)

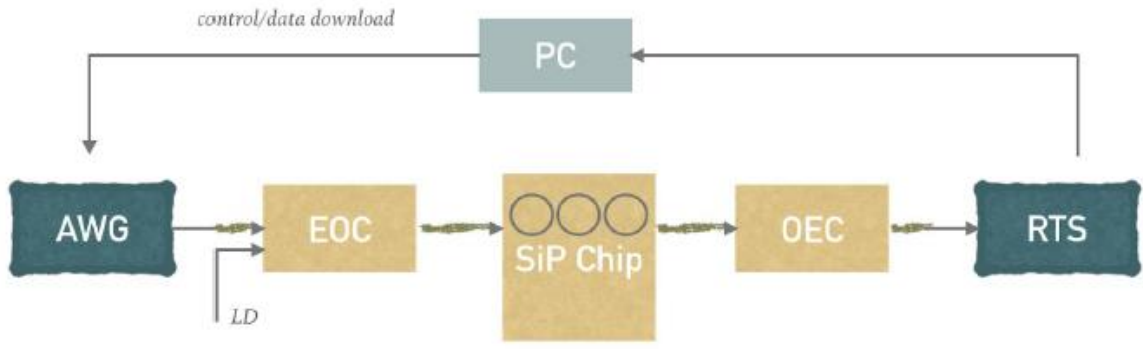


Figure 2: block diagram demonstrating the link in an optical network

**INDUSTRIAL
ENGINEERING &
OPERATIONS RESEARCH
COMPUTER SCIENCE**

Football Simulator 2019

*Thomas Mecattaf, Mohnish Chakravarti,
Cameron Terry
Advisor: Prof. Hardeep Johar*

The goal of this project is to create a recommendation system for coaches to use on their players on a daily basis, such as to provide detailed insights on what areas of his game each player should improve in training. These insights are extremely specific, as they take into account the opponent the team is facing, the teammates a specific player will play alongside with, and the match-day conditions the player will be exposed to.

Fundamentally, we view a player's training regime as an optimization problem for the coach: there are many areas of the game to improve in a player, but a limited time such that crucial choices must be made to prioritize regions of improvement. Hence, if we can create a model that points out the best points to focus on, we are indeed optimizing the training regime of a player.

To do so, we scrape multiple datasets: first, the FIFA video game ratings for each player, which include detailed stats (between 0-100) that describe their physical and mental attributes, and in-game instincts. The second dataset is a list of in-game performance of each team (from whoscored.com). For the sake of this proof-of-concept, we focus only on the English Premier League.

We conduct an analysis on the entire season performance, to see what factors have the most impact on performance, what are the attributes that have the biggest influence on a game for individual players, and what the ratings that distinguish player types are.

Then, after this preliminary study, we run a LASSO regression relating the make-up of a team (11 vs 11 players) to the resulting game performance. In our case, very detailed statistics are available for 4 seasons in total, so we have more than 1600 games at our disposal. We are training an algorithm in which we feed it each player's statistics, and it outputs a predicted in-game performance.

Finally, for each player, we would vary a feature by +1 compared to the original ratings, leaving all other features equal for all other players. We then run that for all the features of that player, and see the ones which have the biggest "positive delta" impact on the game. This would allow us to pinpoint what feature the coach has to focus on while training his players for this specific game.

References:

- [1] Junyuan Gao, [Predicting Premier League Final Points and Rank Using Linear Modeling Techniques](#)
- [2] Suraj Keshri, Min-hwan On, Garud Iyengar, [Optimal Trajectory based Player's ability in NBA](#)
- [3] Rory P. Bunker, Fadi Thabtah, [A machine learning framework for sport result prediction](#)

Predicting Crop Yield in North America: Modeling Corn Hybrid Performance and Farmer Centered Pipelines

*Alysha Hudson, Ara Peterson, David Reiss-
Mello, Joshua Lederer
IEOR Hardeep Johar*

The United Nations project the world population will reach 10 billion in the year 2056, yet our world is running out of cropland Ñ land needed to produce food. And we're currently using our arable land and water 50 percent faster than the planet can sustain. (Syngenta, 2018) At the same time, the crops farmers plant face an unprecedented set of obstacles due to increasingly limited growing conditions and climate change. We are thus faced with the pressing question: how can we enable our global population to grow enough food to meet world demand?

Corn is one of the key crops looked at and bred by scientists to aid in solving the food sufficiency challenge. Each year, breeders create several experimental hybrids and tests them across a wide range of environments. Historically, the high-growth hybrids are identified purely through trial and error. This process can take up to 10 years. By creating accurate models that can predict performance, we could severely decrease the amount of time needed to test and improve on strain variations. This report looks to aggregate environmental data to find useful metrics representing stresses encountered by corn throughout a growing season. e propose that these metrics can be used to discriminate between hybrids tolerant and susceptible to the stresses they represent. Some potential environmental stresses that can have a negative effect on yield are poor weather (heat, drought, cold, etc.), soil lacking nutrients, insect damage or pathogens.

The degree of each stress and how resistant a particular hybrid is to the stresses encountered will determine how much the yield is impacted. Furthermore, individual farmers benefit from having access to this type of information because they can better manage risk across their acres.

The data was preprocessed in python using sci-kit learn. Principal component analysis was performed to understand the impact of the feature vector on the yield. K-means clustering was used to decide on the number of "like" environments in the set of over 2,000 hybrid environment combinations.

The data was then fit with multiple regression model. 10-fold cross-validation of a random forest regression was found to be ideal. The model was trained on each individual hybrid and used to predict a 95% CI of yield. This yield was tested under various stressors and the top 5 hybrids per environment cluster were identified

References

- Adee, E., Roozeboom, K., Balboa, G. R., Schlegel, A., & Ciampitti, I. A. (2016). Drought-Tolerant Corn Hybrids Yield More in Drought-Stressed Environments with No Penalty in Non-stressed Environments. *Frontiers in Plant Science*, 7, 1534.
<http://doi.org/10.3389/fpls.2016.01534>
- Hengl T, Mendes de Jesus J, Heuvelink GBM, Ruiperez Gonzalez M, Kilibarda M, Blagotić A, et al. (2017) SoilGrids250m: Global gridded soil information based on machine learning. *PLoS ONE* 12(2): e0169748.
<https://doi.org/10.1371/journal.pone.0169748>
- Thornton, P.E., M.M. Thornton, B.W. Mayer, N. Wilhelmi, Y. Wei, R. Devarakonda, and R.B. Cook. (2014). Daymet: Daily Surface Weather Data on a 1-km Grid for North America, Version 2. ORNL DAAC, Oak Ridge, Tennessee, USA.
<http://dx.doi.org/10.3334/ORNLDAAC/121>

MECHANICAL ENGINEERING

PreSpice - Automated Spice Dispenser

Sara Cummings, Connor Johnston, Josh Katz, Brandon Kubick, David Reyes
Advisor: Josh Browne

Modern trends in American lifestyles have led to a decrease in home cooking, costing Americans thousands according to USA TODAY [1]. While many justify this spending in exchange for time saved, we interviewed potential customers and found that it was not only the time and mess that discouraged individuals from cooking, but simply the unawareness of what spices they had and how to use them.

Our group decided to address these customer needs by creating the PreSpice. The PreSpice is not only an automated spice dispenser that reduces the mess and guesswork associated with cooking, but also a cooking companion. By keeping track of the user's dried spices and offering recipe inspiration based on user input, the PreSpice introduces the user to new and exciting flavor combinations. These design goals were addressed by our team through integrating hardware and software: making this project just as much a programming challenge as it was an engineering design challenge.

From a hardware perspective, we needed to create a device that would store ten different spices (the number we found to be regularly used by a home chef), and dispense them precisely without cross-contamination. Additionally, it was critical to our design that the user be able to refill containers when they become low and swap out spices as they see fit. Sensors were also utilized to accurately control the hardware, including the implementation of hall effect sensors and photoresistors.

Currently, the device was made to abide by ANSI standards for engineering drawings and design. Additionally, future

container designs will follow FDA regulations to satisfy material requirements due to them being in contact with food. The containers will also avoid sharp angles to satisfy the FDA's cleanability requirement.

Extensive software was created to generate a user-friendly interface. This is displayed on a touch screen that has been integrated into the front of the PreSpice. Here, the user can select pre-programmed recipes or dispense spices individually. The amount of each spice can be adjusted by the user and saved as their custom version of the recipe. Once spices are loaded into the PreSpice, an on-board microcontroller cross-references the spices with recipes stored in the database to determine what can be made by the user.

Our vision is to create a kitchen appliance that makes home-cooked meals more accessible. Through our research, we have found this to be a gap in the kitchen appliance market, as measuring technology has never been successfully automated on a small scale. Though our product is currently only a senior design project, we are pursuing a patent and may continue development in the future.

References:

[1] Martin, Emmie. "90% Of Americans Don't like to Cook - and It's Costing Them Thousands Each Year." *USA Today*, Gannett Satellite Information Network, Sept. 2017

InstaSorg

Quincy Delp, Yifei Tian, Jason Fan, Chengke Fan,
Victoria Wang
Advisor: Arvind Narayanaswamy

Sorghum is a cereal grain, like oats, rice and wheat, which is grown around the world. For several reasons, it is a promising candidate for increased production over the next decade. It is gluten free. It contains a different (and arguably superior) nutrient profile than other commonly consumed grains¹. Most importantly, it is resistant to water logging and drought. If we are trending towards precipitation being less consistent, this is an essential trait. It is consumed by people regularly in Sub-Saharan Africa and by livestock in the US but not by the growing global middle class in the US, China, or India. We believe this is because of its long cooking time – on a stove, sorghum takes 60 to 90 minutes to cook. If meal preparation occurs after coming home from work, this time frame simply isn't feasible. Our aim is to make a device which prepares quick-cooking sorghum that can be cooked on the stove or in the microwave in 10 minutes or less.

To outline the specifications of our device we performed a series of tests and calculations. Specifically, we needed to isolate a pre-cooking temperature, pressure and duration, the amount of torque required to actuate the flaking device, and the heat, wind speed and duration of our drying device. We are using an InstaPot to pre-cook the sorghum, which we operate at a temperature of 100 C and pressure of 70-80 kPa for a duration of 5 minutes to achieve a sufficiently high moisture content. We required 0.8 Nm of Torque and 5.024 W of Power from the driving motor of the mill. The NEMA-23 motor we ordered is capable of 3.0 Nm and operates at up to 50.4 W. Finally, for a target batch-size of 50 grams and based on a calculated mass transfer coefficient of 0.00717 kg/m²s, we require our fan and heating element to be powered for 6 minutes and 20 seconds to achieve a moisture ratio of 0.13, the safe limit for grain storage.

Our design builds on existing models for quick-cooking cereal.² It differs in a few key ways. First, we use knurled aluminum rather than a flat-faced cylinder to perform flaking. This creates a tighter grip with the grain and is able to create a larger surface area, reducing the rehydration time required. Second, rather than cooking the grain after

flaking, we immediately move to dry³. While we risk uneven starch gelatinization, we save tremendous amounts of energy from the second cooking step and believe that starch is fully gelatinized by the pressure cooking.

The device is manufactured in a few modules. The flaking module (detachable) contains an aluminum base plate, on which is mounted the stepper motor and driver, knurled rollers, and microcontroller. The main housing was made using aluminum t-slotted bars and food safe acrylic stenciled in a laser cutter. The basket (detachable) is made using stainless steel screen and hangs on two steel dowels. The drying elements are made using a nichrome resistor and DC high-speed motor. Finally, there is a screen which replaces the flaking module during drying to prevent grains from flying out of the device.

We hope that by decreasing the cooking time of this nutrient rich, gluten free, resilient crop, Sorghum will gain prominence in and beyond the sustainable agriculture community.

References

- ¹Sorghum:<https://ndb.nal.usda.gov/ndb/foods/show/20067> Oats:
<https://ndb.nal.usda.gov/ndb/foods/show/45342702>
Rice:
<https://ndb.nal.usda.gov/ndb/foods/show/45260158>
- ² Miller, F. J. (1957). US Patent No. US2930697A. Retrieved from <https://patents.google.com/patent/US2930293A>
- ³ Glenn, Gregory M. and Johnston, Ruth K. (1992) "Mechanical Properties of Starch, Protein and Endosperm and Their Relationship to Hardness in Wheat," Food Structure: Vol. 11: No. 3, Article 1.



*Peter Hidley, Chase Pipkin, Travis Pulliam,
Nathaniel Fisher
Advisor: Joshua Browne*

Our goal is to design and create an automated, motorized stabilization system for Citi Bike. Our system is made up of two rolling stabilization legs that thread onto both sides of the rear axle (similar to training wheels). Each aluminum leg is powered by a DC motor integrated with a self-locking worm gear system, programmed to rotationally retract and deploy at certain speed thresholds. As a Citi Bike rider slows to a stop, our legs will deploy at approximately 3.5 mph, thanks to a speed sensor, preventing the bike from toppling over and eliminating the need for the rider to take their feet of the pedals. Similarly, as the rider begins pedalling, our legs will retract at the same 3.5 mph speed threshold, giving the rider a conventional bicycling experience.

Project Rationale:

The motivation behind this design is to provide a safer and more feasible ride for those who use Citi Bike as a means of transportation, or may want to but are unable because of injury or disability [1]. With over 60 million total rides, Citi Bike was a viable company to partner with to target an unmet need in today's society [2]. In a city like New York, riders will have to stop multiple times whether that be for stop lights, stop signs, or something unpredictable. Implementing our design will provide a more stable and stress-free riding experience. As fellow bike enthusiasts, we wish to share the love of bicycle riding with an increasingly broader population [3].

Final Design:

Our design has undergone many iterations before arriving at the current state, which is shown in Figures 1-4. We wanted to create a mechanism that would provide the automatic

stabilization desired while still being aesthetically pleasing, lightweight, and functional. We implemented a worm gear driving system for its self-locking geometry and for its overall design simplicity. As shown in Figure 2, the motor is recessed into the leg and secured by hose clamps to align our drive and worm gear. We strategically placed holes to minimize weight and retain strength. The wheels are slightly elevated off the ground, similar to traditional training wheels, allowing full deployment of leg without interference with the ground. An arduino and GPS speed sensor control the deployment and retraction of the legs, which take approximately one second, ensuring stabilization before complete stopping and destabilization occurs. Figures 3-4 show the legs deployed and retracted, respectively, on a Citi Bike to provide a complete image of our implemented design. By incorporating a lithium battery, we can achieve a lightweight source of power as well as provide a significant number of deployment - retraction cycles on a single charge.

References

- [1] Mark Birthingam. Summer: a Season for Ankle Sprains. Boulder Medical Center, 11 July 2017.
- [2] Motivate. New Milestone: Citi Bike Reaches 60 Million rides Since Launch. 6 June 2018.
- [3] Winnie Hu. More New Yorkers Opting For Life in the Bike Lane. The New York Times, 30 July 2017.

Figure 1: Front View of Leg



Figure 3: Stabilization Legs Deployed



Figure 2: Isometric View of Leg



Figure 4: Stabilization Legs Retracted



Note: all figures do not include the control unit, which will be placed between the seat post and the rear wheel, or a housing that will encase the gear system

IoT Tensegrity Tumbleweed

*Breanna Johnson, Leonardo Costa, Luke Gile,
Steven Hyland
Advisor: Dr. Josh Browne*

The Tumbleweed is a tensegrity structure that utilizes Internet of Things (IoT) controlled DC motors to induce rolling motion. Tensegrity structures are a cheap, compressible, durable and lightweight solution to many of the challenges faced by the space exploration and emergency services industries.

Tensegrity structures are composed of members (beams/struts) held in compression by a series of cables in tension. These structures come in a variety of shapes that differ in strut number. For the purposes of this project, the size pursued was a six strut assembly to allow for a spherical design. After deciding upon the robot's structure, actuation was considered next. In order to actuate in the full 360° range of motion, a single DC motor and spool was attached to each strut. Kevlar string was then attached to each spool, threaded through an eye hook at the end of each strut and then passed and threaded onto another separate strut. The motor and spool system reels in the kevlar, bringing two adjacent wired struts together. Once the struts come closer, the center of mass shifts from its original position - at the center of the sphere - causing the assembly to move in the direction of which the struts had been pulled together. This repeated motion allows the robot to 'tumble' through an environment. To maintain the distance between each strut when not being actuated, a neoprene rubber netting is used. This rubber lattice ensures symmetric and equal tension throughout the spherical robot while allowing for movement.

Deployability of structures is a major concern for space exploration. The ability to withstand impact when dropped from large heights is a defining characteristic of tensegrity structures. With the symmetric compressive and tensile nature of the tensegrity structure, it assumes a shock-absorbing mechanism. Due to the lack of touching compressed elements (struts), the robot is able to fully compress when dropped from any height and then return to a relaxed state. The rubber lattice and 'floating' struts ensure that the robot does not experience a

point of force concentration or breaking failure, thus allowing for a robust robot.

To control the DC motors and reduce wire congestion and tangling, wireless control capabilities have been utilized. Originally, a single Arduino was used to control all motors and was located on-board. Our second electronics system design utilizes a WiFi-enabled Photon Board equipped on each strut, with a 'central brain' Photon Board located off-board to control the other Photon Boards. The Wi-Fi capabilities allow for each Photon to communicate through publisher/subscriber functions and control each strut without being wired to one another. This modular design also enables ease in part replacement and rapid prototyping.

3D printed mid-caps are used to encapsulate both the actuation and electronic components on each strut. These mid-caps ensure that all hardware is properly housed and remains on-board even when dropped. In each mid-cap we used a Photon Board micro-controller, a 5V regulator, an H-bridge circuit, a 9V and a 3.7V battery to power different components, a DC micro geared motor with an attached spool.

The uncertain terrain encountered in space exploration is a major concern for deployed vehicles. Our tensegrity robot is capable of combating these issues via advanced locomotion and climbing abilities. In addition, its structure allows for easy compartmentalization, heavy payload resistance, as well as fast and low-cost production. Hence, tensegrity systems are an alternative for the future in the space exploration industry.

Shred-It

Riley Greene, Racquel Glickman, Molly Hazlehurst

Advisor: Joshua Browne

Millions of people eat collard greens in Kenya every single day for sustenance. The vegetable is widespread throughout the country, as it is plentiful and cheap. In Africa where dietary variety is a luxury, many people are eating this vegetable almost exclusively. The traditional preparation of the vegetable is extremely time consuming as it requires hand rolling the large leaves into a tight bundle and thinly slicing strips into pieces that are no more than 0.25cm wide.

Currently there isn't a thin slicing leaf cutting technology on the market in the United States or otherwise. We believe to have a novel solution to the problem that can help to rapidly expedite the leaf cutting process for millions of people in Kenya. The goal of the project is to create an enclosed tabletop shredder for collard greens that makes their preparation more efficient, more safe, and more sanitary.

As a team we felt that it was vital our solution was cleanable, and made with parts that could be easily replaced as necessary. Our solution implements six rods that can be removed as necessary via a system of eight shaft couplers and four spring pins as shown in Figure 1. The shredder was also made with kitchen conditions in mind in terms of size and water proofing. We recognized that the collard greens would likely be wet as they entered the device so using corrosion resistant materials was paramount. In addition to proper material selection, the electronics which drive the blades needed to be effectively separated from the cutting action due to the presence of water.

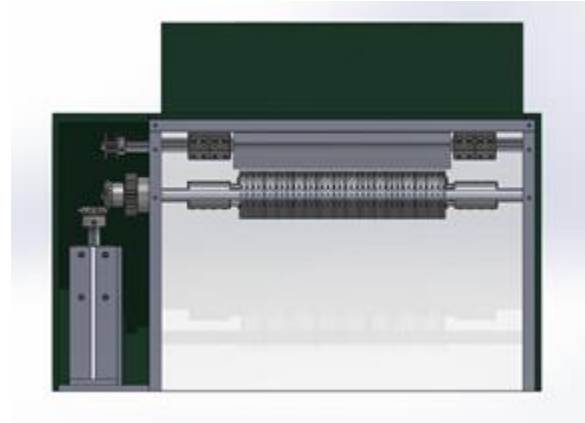


Figure 1: Side view of the shredder showing inner mechanisms

Another consideration that was factored into our design was the fact that our device needed to be food safe according to standards put into place by the United States Department of Agriculture Food Safety and Inspection Service (USDA FSIS), the Kenya Bureau of Standards (KEBS), and the International Standards Organization (ISO). As our budget was limited for the project at this stage our project is currently not food safe and simply being used as a proof of concept. However, every part being used in our shredder has a food safe equivalent, and implementing those solutions moving forward does not pose a problem.

Looking forward as a team we are currently in collaboration with a SIPA student from Kenya who has been keen to bring this project to market. If possible and when necessary we can make design modifications to powering the machine via a mechanical hand-crank or solar power. As approximately half of Kenya is not on the grid - this may increase the widespread usage of the device.

iPothecary

*Yeil Choi, Christian Puerta, Elijah Shultz and
Cory Ye*

Advisor: Josh Browne

For many people, especially those who are elderly, pills and medication is a natural fact of life. A large number of those people are highly dependent on said pills. For them, overdosing or even underdosing can become a hazard. Many pharmacies sell sorted containers for their pills but it's easy to forget or even lose these boxes. Sorting the pills themselves can be tedious work. These days, there are many technological solutions to this problem involving large machines and dispensers, but many of them are expensive, complex, slow or even unsafe.

It's not hard to see why pills are increasingly becoming an issue for many people. Prescription volumes have nearly doubled from 2.4 million to 4.4 million from 1997 to 2016 according to a 2017 Consumer Reports study¹. That same study found that about 55% of Americans take prescription medications and 75% take over the counter drugs regularly. On average adults have 4 prescriptions, and this number increases drastically with age. A prevalent issue in the medical community is medication non-adherence which has been a well-documented and longstanding problem, where a patient can become careless and forget to take a prescription.²

But pills are not easy to deliver. Even "simple" medications like vitamins and painkillers are often taken sporadically and add to the problem. Once a large number of pills come into the picture, the issue grows in complexity. Different kinds of medicines have to be taken in different quantities and at different time intervals. Organization becomes extremely difficult very quickly, as remembering what to take, when to take it, and when the last medication was taken is complicated. Such as it is that non-adherence becomes a problem. With older family members, medical care becomes a multi-person job, which can be extremely tedious. Ensuring that the correct medication is taken at all hours can become invasive to the lives of family members as well as being time consuming.

To solve this pervasive problem, we have spent this past year creating the iPothecary. With this machine, we intend to simplify the lives of both patient and caregiver through reliable automated pill dispensation along with software tools to help in administering medication needs. The iPothecary brings convenience by taking away the need to sort different pills individually and by allowing both users and caretakers to set reminders to ingest the medication required throughout the day. A total of 9 separate containers live inside of the machine, each holding a single type of medication. To ensure the privacy of the user and the security of the pills, we have added in a RFID chip system that requires users to scan before they can begin taking out their pills. In addition, the machine makes use of the Internet of Things to ensure accuracy of times and user information. We promise that this machine is simple, easy to use and will make the lives of those who need pills better.

References

1. Carr, Teresa. "Too Many Meds? America's Love Affair With Prescription Medication." *Consumer Reports*, 3 Aug. 2017
2. Gadkari, Abhijit S, and Colleen A McHorney. "Unintentional Non-Adherence to Chronic Prescription Medications: How Unintentional Is It Really?" *BMC Health Services Research*, BioMed Central, 14 June 2012

The Ark

By AütoFlöt

Kirsten McNeill, Andrew Moshova , Liam Dwyer, Patrick Naughton, Mark Hellinger

During Hurricane Harvey alone, it is estimated that as many as one million cars in the Houston metro area were destroyed. Floodwaters can corrode a car's metal components; cause exhaust system failure; engine seizure and overheating; transmission failure; short-circuiting of wires; computer malfunctions; inoperative lights and dashboard; warped/rusted brakes and rotors; ABS malfunctions; airbag/restraint system failures; interior contamination; moldy seats/fabric; and bacteria in the car's ventilation system.

The Ark seeks to address the gap in technical solutions to vehicular flood protection and is currently the only known device that is designed to effectively and affordably protect a car from floodwaters. This project aims to manufacture a device that is durable; easily stored and transported; quickly and easily deployed; and provides stability and flotation for multiple days. The Ark consists of four modular, inflatable sections which attach to each wheel of a vehicle via metal chocks and straps. In its intended use case, a user attaches wheel chocks to each tire, clips inflatable pontoons to each set of chocks, connects the inflation device to the car's battery, and then inflates the device. The car would then be tethered to a suitable structure with attachment points at each chock prior to flooding. Weighing around 120 pounds for all components, with each component weighing no more than 20 pounds, and

costing around \$610 for a scale model, The Ark's design is transportable, easily deployable, and reasonably priced for an early prototype. The Ark's design consists of very few carefully designed, yet simple, components, and is modular to allow future design flexibility for multiple vehicle types.

A Non-slip Continuously Variable Transmission for a Bicycle

*Max Holschuh, Nikolay Ionkin, MingxinJia,
Graham Maxwell, and William Zhang
Advisor: Joshua Browne*

Bicycles are some of the most popular vehicles in the world due to their low cost and convenience. Nearly all bicycles utilize a single gear ratio or a derailleur design that has a number of discrete gear ratios. Therefore, any adjustments to increase the performance or comfort of a bicycle are significant.

Columbia Vector Technologies has developed a continuously variable transmission (CVT) that is mounted and has been tested on a bicycle. The target audience of the system is an end-user who uses their bicycle for recreational riding or commuting in city terrain. The advantages a CVT provides over a traditional derailleur system is the lack of intermittent shifting loss and a simplified shifting process for the operator. In the past, several CVT designs have been proposed, but have failed to become standardized due to various obstacles, namely the inability to match a gear range comparable to a derailleur system.

The novel CVT design proposed aims to solve this issue by eliminating the commonly accepted use of belts in CVTs, which slip at high torques, and instead utilizes a ratcheting mechanism. The gear ratio is varied by changing the moment applied to a lever arm that drives an output crank. This lever arm only engages with the output crank in the forward direction as it moves back and forth. In addition, the non-constant RPM output can be used to the advantage of pedaling. All CVT components and the bicycle are either purchased or fabricated within a budget of \$1000 and an extensive engineering analysis and manufacturing plan is provided to ensure

a robust design that fits within a typical bicycle frame.

ASME codes/standards relevant to dimensioning, tolerances, and other design-related aspects have guided our process. In addition, ISO 4210 pertains to safety requirements for bicycles and we have incorporated this into our design.

FSAE EV Systems Integration

*Team FAHK: Fernando A. Pascual, Austen Paris, Henry Tucher, Katherine Guan
Advisor: Prof. Josh Browne*

For our senior design project we are building Columbia University's first electric racecar for Formula SAE intercollegiate racing. Our project scope includes integrating the electric vehicle functional systems into the chassis of an existing FSAE internal combustion racecar as well as coordinating and leading the FSAE EV team in all mechanical engineering aspects of the racecar. Four key mechanical design challenges for this project include battery accumulator design, motor packaging, mechanical drivetrain implementation, and structural chassis design. The team is also designing two cooling systems for electrical components as part of a separate Electrical Vehicle Drivetrain Design class.

Design projects for EV Drivetrain Design Class include motor and inverter cooling which will be completed under the scope of the EV Drivetrain class by Fernando Pascual, and battery cooling thermal analysis to be completed by Austen Paris and Katherine Guan. Other design projects have been delegated to team members or reserved for later in the competition lead up. A new steering wheel with a larger display is being designed by a mech-e team member, for which Henry Tucher is designing the display in addition to the Structural Equivalency Sheet (SES).

Because this is Columbia's first attempt at building an electric racecar for FSAE, the team seeks to achieve basic moving vehicle operation and establish a benchmark for successive teams. A further goal is for the vehicle to pass FSAE technical inspection and compete at FSAE North in Barrie, Ontario in 47 days. This report details our designs, ideation, and engineering

analysis to validate our design's expected performance. Through this project, we aspire to promote sustainable transportation and the future of electric vehicles on campus.

CAD models and fabrication progress can be referenced in **Figures**.

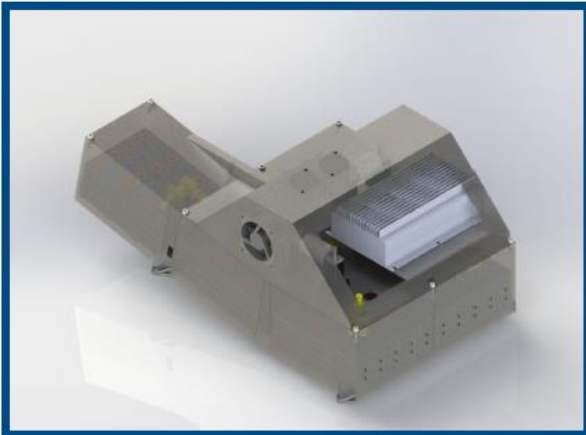
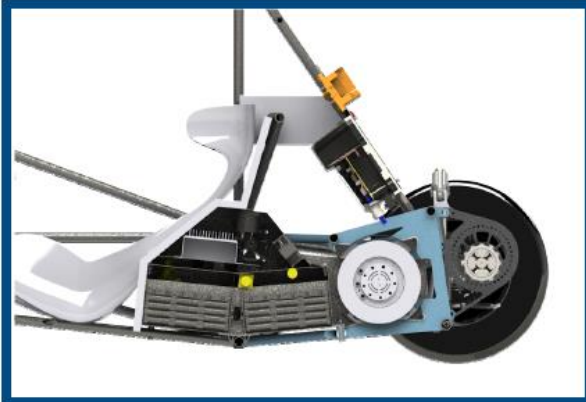
References

We began research for our E-FSAE project through a website review of University of Pennsylvania's standout FSAE Electric team [1]. Penn's website and documentation yielded a framework to reference for the design considerations of our own car. We found Penn's 2016-2017 REV3 electric car runs a single motor for rear-wheel drive utilizing an Enstroj Emrax 207 MV motor similar to the Emrax 208 motor we will use [2]. The second principal source we consulted from our online search was the Formula SAE rulebook, which documents comprehensive guidelines for FSAE design, safety, and competition, with a section devoted specifically to electric vehicles [3].

We also found the University of Wisconsin's FSAE Electric team's paper detailing accumulator design particularly useful [4]. Lastly, a paper published by Toyota describes using forced convection to air-cool batteries, which we consulted when considering the ventilation and cooling through our accumulator design [5].

1. <http://www.pennelectricracing.com/r-ev3>
2. Emrax 208 Technical Data Table
3. Formula SAE Rules 2019 - FSAEOnline.com
4. Wisconsin Accumulator Design
5. <https://patents.google.com/patent/US5937664A/en>

Figures
CAD Models



Fabrication Progress



Shoe Tying Robot

Arturo Mori, Cesar Trujillo, Eric Li, Rafael Corrales Fatou

Robotic dexterity is a complex skill to achieve. Today, researchers are pushing the limits with the goal of increasing dexterity. In the shoe industry, increasing dexterity would mean an increase in supply chain. According to the CEO of Adidas “The biggest challenge the shoe industry has is how do you create a robot that puts the lace into the shoe” [1].

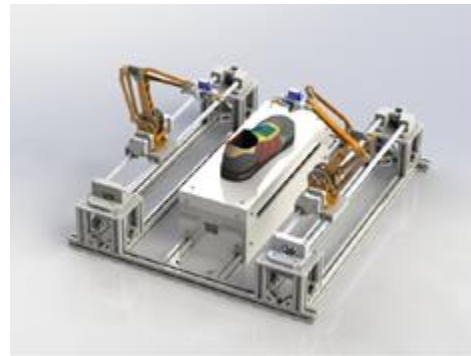
A study published by AVG technologies which surveyed families across the USA, Canada, and the EU5, showed that toddlers (2-5years old) are more likely to know how to play a basic computer game than be able to tie their shoes [2]. Today, there are industry leading companies such as Nike and Puma conducting R&D into self-tying shoes with the applications varying from an everyday shoe to professional sports.

Our project takes a different approach to this rising problem. The goal of this project is to create the first robot that will be able to different types of shoes instead of one single shoe. With the incorporation of different sensors, the possibility of a closed loop system is no longer unattainable. What sets this apart from the previous shoe tying robots is that this has the goal of incorporating practical usability compared to previous attempts which did not allow a user to have the shoe on.

Codes and Standards:

The basis of our mechanism is for it to be produced through adaptive manufacturing capabilities. To achieve this, we are following ASTM52910 and Y14.5 when designing components. For 3D printing of our components, we follow ASME Y14.46-20 1 7 standard.

Render:



References

- [1] Bain, Marc. “One Very Basic Job in Sneaker Manufacturing Is Testing the Limits of Automation.” Quartz, Quartz, 24 Apr. 2017, qz.com/966882/robots-cant-lace-shoes-so-sneaker-production-cant-be-fully-automated-just-yet/.
- [2] PR, AVG. “Digital Abilities Overtake Key Development Milestones for Today’s Connected Children.” Digital Abilities Overtake Key Development Milestones for Today's Connected Children, AVG, 3 Feb. 2014, now.avg.com/digital-abilities-overtake-key-development-milestones-for-todays-connected-children.

PLASTICS

*Thomas Orr, Aaron Thompson,
Jose Pablo Rueda Molina, Erik Boyle
Advisor: Josh Browne*

Our project drew inspiration from work done at MIT on printing free-form meshes into gel like material. This gets away from a layer-based process and thus allows for considerably faster printing processes. Additionally, the beam size being used is several millimeters in magnitude, allowing for the creation of robust structural shapes. However, it is currently limited to resin type materials. This limits fundamental strength as either the resin is kept soft until it rebonds (which could be at any point in the future of the printing process) or the resin bond isn't fully reptated (entangled with the existing polymer molecules). This led us to the ideation of a thermoplastic variation of the gel printing process, replacing the irreversible cure hardening process with a reversible melt hardening process.

On the hot end side this would mirror the approach used by conventional FDM: filament is pushed through a hot region and then extruded onto existing structures. Upon extrusion, it bonds to existing material through a process of reptation. However, as limitations in current approaches to bridging (bonding between two pillars in a print with no underlying support) in FDM show, it is impossible to print over nothing without some high degree of sagging. To circumvent this issue we propose to rapidly cool the polymer by passing chilled fluid over it in a small surface layer. We have tested different coolants, yielding variable results. The motions of the extruder can be hardcoded or can be obtained through a path-finding algorithm that necessarily takes into account the position of the already-printed beams and trusses, to avoid collisions with these. The geometry of the head of the extruder, along

with the unorthodox build-plate necessitate a non-trivial path-finding algorithm, but one that yields many possibilities when it comes to creating 3D structures. Thus, our project revolutionizes the field of digital manufacturing.

References:

Crump, S. S. (1989). U.S. Patent No. US5121329A. Washington, DC: U.S. Patent and Trademark Office.

Gordon, M. C. (2015). U.S. Patent No. US20160207263A1. Washington, DC: U.S. Patent and Trademark Office.

Kanada, Y. (2015). U.S. Patent No. US 20150.039 113A1. Washington, DC: U.S. Patent and Trademark Office.

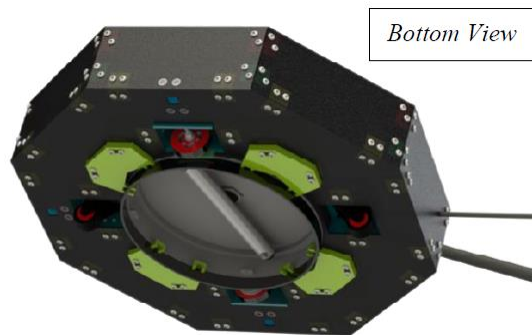
Mueller, S., Im, S., Gurevich, S., Teibrich, A., Pfisterer, L., Guimbretière, F. & Baudisch, P. (2014, October 5). WirePrint: 3D Printed Previews for Fast Prototyping. Retrieved November 9, 2018, from

<http://groups.csail.mit.edu/hcie/files/research-projects/wireprint/2014-uist-wireprint-paper.pdf>

CulpeoWASH

*Team Hydraulic Foxtrot: Adeel Ahmad,
Onur Calikusu, Christopher Fryer, Charles
Johnson
Advisor: Joshua Browne*

Our project centers around building an automated pressure washing robot for ground surface applications. Pressure washing a surface is often a strenuous and tedious task requiring a lot of effort and time. This especially holds true during a hot summer day and/or when a very large surface needs to be cleaned. We are introducing an automated platform built around an existing surface cleaner, as shown below, to alleviate this problem. This will prove to be useful in various environments, including but not limited to, driveways, decks, and tennis courts.

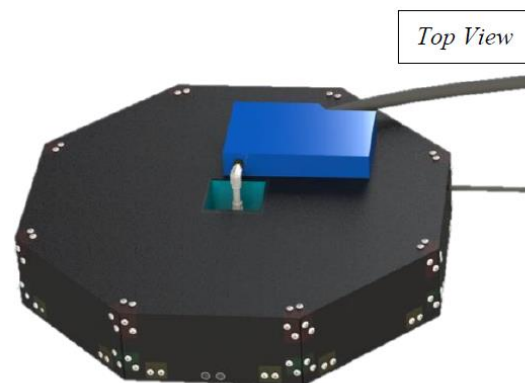


CulpeoWASH utilizes various sensors to navigate around its environment and ensure an even wash. The combination of distance sensors, ultrasonic sensors, and a digital compass ensure that it operates in an optimal fashion. The placement of distance centers around the chassis of the robot ensures that no collisions occur during the robot's operation and that it does not fall off of the deck that it is washing. The digital compass is used for the robot to maintain a straight-line motion while implementing PID control to stay on track, even on rough terrain. The robot's body will be made of acrylic that is sealed with a waterproof caulk so water does

not leak into the electronics system. Various electronic components are also placed in waterproof seals so that no damage occurs to the system during operation. Laser cutting and 3D printing are the main methods of manufacturing, providing an affordable overall cost.

In terms of operation, the user places CulpeoWASH in a corner and connects it to a power and water source. The user verifies the motion and parameters of the wash such that an optimal route for the robot is determined. It then begins its motion in a zig-zag pattern, providing a consistent clean. Because pressurized water is a potential hazard, safety measures are implemented if the robot happens to run into any issue. For example, if the robot is raised or toppled during operation, an accelerometer communicates with the robot to stop all motor functions and cut off the water supply.

Overall, CulpeoWASH has various commercial applications that will greatly benefit homeowners. It provides an automated platform for a tedious task and will require minimal supervision. With its unique navigation algorithm and sensing capabilities, the realm of pressure washing will be revolutionized.



Card Dealer 3000

*Andrew DePerro, Connor Finn, John
Michael Long, Brian Nicholas
Advisor: Dr. Joshua Browne*

The Card Dealer 3000 is a compact, table-sized, card dealing machine. To begin your hours of card game fun, simply load a pre-shuffled deck of cards into the machine, select your card game of choice, select the number of players, and the Card Dealer 3000 completes all the tedious dealing work for you! The Card Dealer 3000 features a removable card shoe for easy card deck loading, an efficient flipping mechanism, a ranged card shooter, programmability for a wide array of card games, and the ability to accommodate a variable number of players.

This device has the ability to do anything a casino dealer can do once the card deck is loaded into the shoe. It is equipped with 5 individual systems that combine into one amazing product. The first, and most important system of the Card Dealer 3000 is the user interface. A custom made controller is utilized to house a LCD board to display the options of the device as well as a 9-character keypad to choose the desired options. Once the options have been selected, the Card dealer 3000 is ready to do the rest.

The card picking system is the first mechanism the card travels through. After a shuffled deck is placed into the card shoe and the card shoe is inserted into the device, a stepper motor with a foam grip picks the top card from the deck. This moves the card to the flipping system. The flipping system uses a stepper motor with a timing belt to move the housing in card non-flipping and flipping orientation. In the non-flipping orientation, the card moves from the card shoe to an angled slide that deposits the card to the shooting system. In the flipping orientation, the card moves from the card shoe onto a thin angled arm to flip the card along its stable

axis. The card then flips onto the same angled slide as the non-flip orientation and is deposited to the shooting system.

The shooting system is a two motor system that the card travels through to be dealt out to a player. A stepper motor with a foam gripper pushes the card forward on the angled slide into a compact DC motor. Once the card comes in contact with the spinning rod attached to the DC motor, it is dealt to the player. The compact DC motor has the ability to deal the card to different distances. The final system is the rotating system, which includes a Lazy Susan bearing and a DC motor with an attached encoder. The encoder allows the Card Dealer 3000 to rotate accurately. This is important when the device is dealing to different players. One last unique feature about the Card Dealer 3000 is that it uses RFID technology so that the machine knows what cards are being dealt to the players, but more importantly, it knows what it also has. This is key for certain games to be successful such as Blackjack.

The Card Dealer 3000 is a portable device with a sleek design that will surely impress any guests at your future game night. It brings the casino to you!

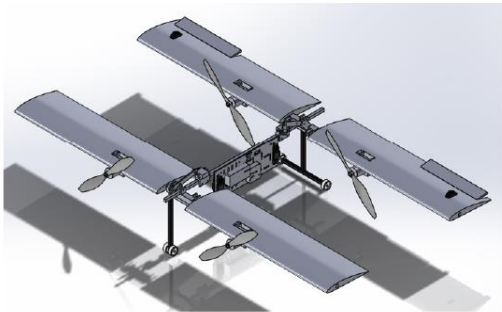
Relevant Standards & Codes:

- ISO 8124-1:2018: Safety of toys -- Part 1: Safety aspects related to mechanical and physical properties
- ISO / ASTM52915 - 16 Standard Specification for Additive Manufacturing

VTOAL Aircraft

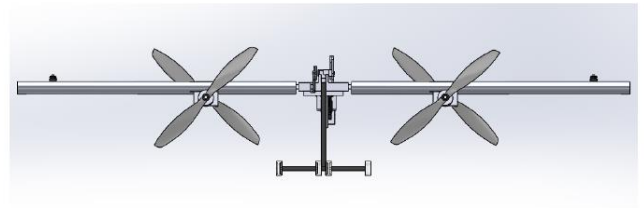
*The Wright Siblings: Simon Anuszczyk,
Rebecca Brunsberg, Haeyeon Jang, John
Pederson, Lily Zhao
Advisor: Josh Browne*

The Swinger is a tandem-wing aircraft capable of both VTOL (Vertical Take-Off and Landing) and airplane flight through in flight wing rotation, combining the best qualities of a drone with those of an airplane. It has four rotors, four 9.5 inch diameter propellers, and two meter-long foam wings attached with carbon fiber rod.



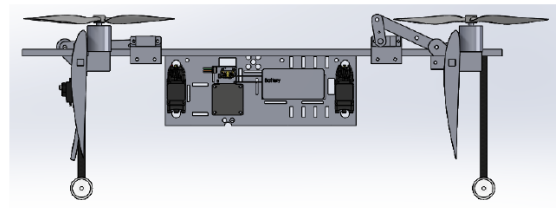
It has two flight modes depicted on the right. It has landing gear, and control surfaces on the back wing to allow for pitch, yaw, and roll.

The craft will take off in drone mode, tilt its wings 90° to change to plane mode, then tilt its wings back 90° to land in drone mode.



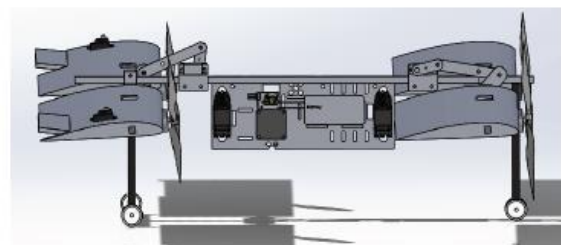
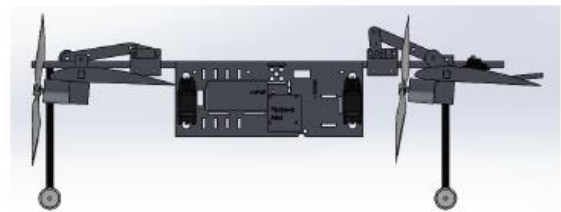
Drone Mode:

Drone mode facilitates VTOL, allowing for the aircraft to take off from and land in a small area without a long runway.



Plane Mode:

Plane mode allows the lift from the wings to aid in maintaining the lower power requirement of an airplane (compared to a drone), allowing us to travel further distances on the same battery life.



Senior Design Expo Team

We would like to thank the following administrators, faculty, and staff with their help in making this year's Senior Design Expo a success.

Leora Brovman, *Associate Dean of Undergraduate Student Affairs and Academic Administration*
Adrieanna Reyes, *Graduate Assistant at Undergraduate Student Affairs & Co-Coordinator*
Dario Vasquez, *Program Specialist & Co-Coordinator*

Applied Physics & Applied Math

Svitlana Samoilina, *Program Coordinator*

Biomedical Engineering

Arthur Autz, *Laboratory Machine Manager*

Aaron Matthew Kyle, *Senior Lecturer in the Discipline of Engineering Design*

Civil Engineering

Tom Panayotidi, *Lecturer in the Discipline of Structural Engineering and Mechanics*

Earth and Environmental Engineering

Robert Farrauto, *Professor of Professional Practice*

Electrical Engineering

David Vallancourt, *Senior Lecturer in the Discipline of Circuits and Systems*

Industrial Engineering and Operations Research

Kristen Maynor, *Academic & Student Affairs Assistant*

Mechanical Engineering

Joshua Browne, *Adjunct Associate Professor*

Robert Stark, *Manager of Instructional Labs*

Communications

Holly Evarts, *Director of Strategic Communications & Media Relations*

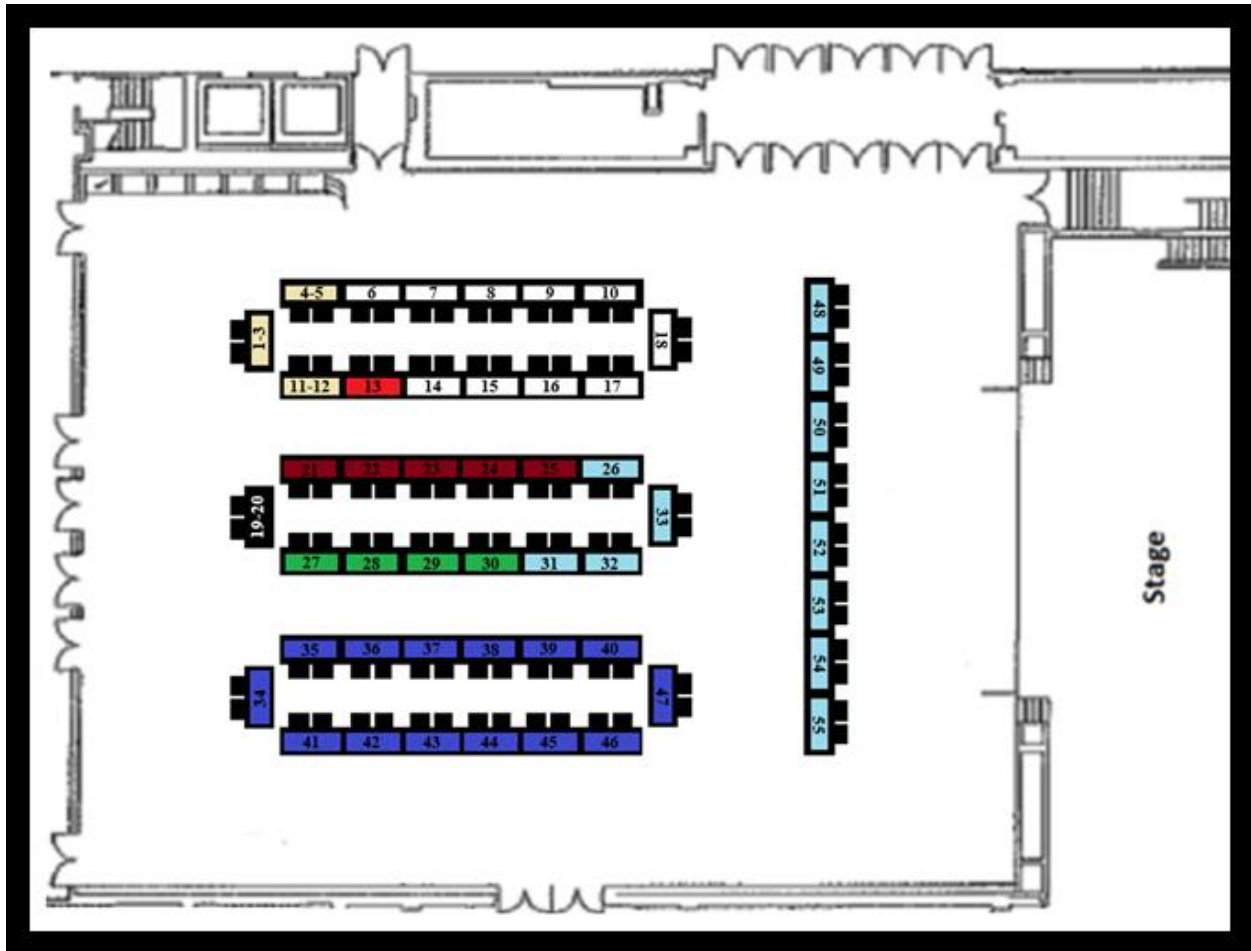
Mindy Farabee, *Associate Director of Communications*

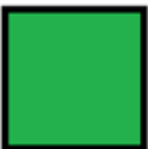
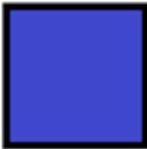
Joanne Hvala, *Senior Director of Communications*

Jane Nisselson, *Associate Director of Multimedia Communications & Designer of 2019 Senior Design Expo Logo*

Alumni Relations

Emma Williams, *Assistant Director of Alumni Relations*



	Applied Physics & Applied Math		Chemical Engineering
	Biomedical Engineering		Industrial Engineering and Operations Research
	Civil Engineering		Electrical Engineering
	Earth & Environmental Engineering		Mechanical Engineering